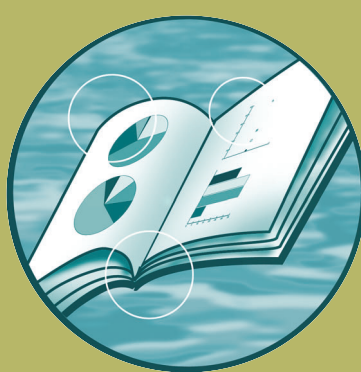
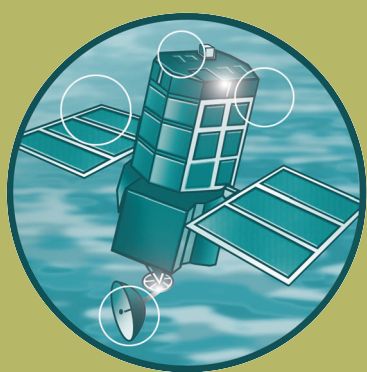


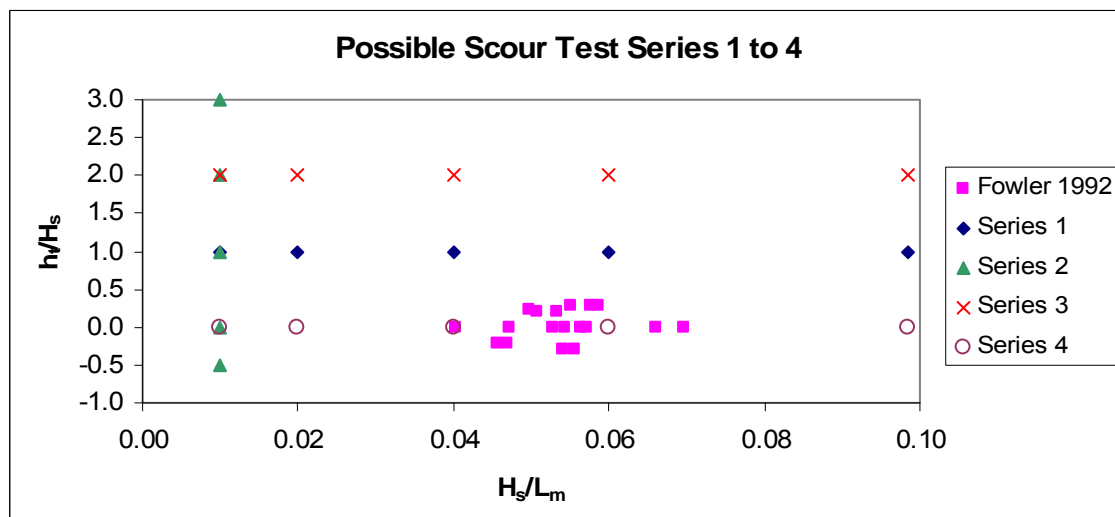
Understanding the lowering of beaches in front of coastal defence structures, Stage 2 Technical Note 2

R&D Project Record FD1927/PR2



Understanding the Lowering of Beaches in front of coastal defence structures, Phase 2

Design of physical model scour tests



Technical Note CBS0726/02



Address and Registered Office: HR Wallingford Ltd. Howbery Park, Wallingford, OXON OX10 8BA
Tel: +44 (0) 1491 835381 Fax: +44 (0) 1491 832233

Registered in England No. 2562099. HR Wallingford is a wholly owned subsidiary of HR Wallingford Group Ltd.

Document Information

| | |
|------------------------------|---|
| Project | Understanding the Lowering of Beaches in front of coastal defence structures, Phase 2 |
| Technical subject | Design of physical model scour tests |
| Client | Department for Environment Food and Rural Affairs |
| Client Representative | Stephen Jenkinson |
| Project No. | CBS0726 |
| Technical Note No. | CBS0726/02 |
| Filename. | CBBS0726-02_design_of_physical_model_scour_tests_V2.0.doc |
| Project Manager | Dr J Sutherland |
| Project Sponsor | Dr RJS Whitehouse |

Document History

| Date | Revision | Prepared | Approved | Authorised | Notes |
|-------------|-----------------|-----------------|-----------------|-------------------|--|
| 20/06/06 | 2.0 | JAS | RJSW | KAP | Defra logo added. Client representative changed. |
| 24/10/05 | 1.0 | JAS | RJSW | KAP | Issued to Defra for review |

HR Wallingford accepts no liability for the use by third parties of results or methods presented here.

The company also stresses that various sections of this document rely on data supplied by or drawn from third party sources. HR Wallingford accepts no liability for loss or damage suffered by the client or third parties as a result of errors or inaccuracies in such third party data

Contents

| | | |
|-------|--|----|
| 1. | Introduction | 1 |
| 2. | Interrogation of NFCDD | 3 |
| 3. | Physical Model Scaling for Scour Tests | 5 |
| 3.1 | Bedload or suspended load? | 6 |
| 3.2 | Bedload Transport Scale Models | 8 |
| 3.3 | Suspended Load Scale Models | 9 |
| 3.4 | Effect of mode of sediment transport | 9 |
| 4. | Prediction of suspension | 11 |
| 5. | Previous suspended sediment transport physical model tests | 13 |
| 5.1 | Xie (1981) | 13 |
| 5.2 | Hughes & Fowler (1991) | 14 |
| 5.3 | Fowler (1992) | 15 |
| 5.3.1 | Drawbacks | 18 |
| 5.4 | SUPERTANK | 19 |
| 5.4.1 | SUPERTANK summary | 22 |
| 5.5 | GWK | 22 |
| 5.6 | Sakakiyama and Kajima (2002) | 23 |
| 5.7 | Summary of suspension modes scour tests | 23 |
| 6. | Physical Model Facility | 27 |
| 7. | Sediment characteristics | 29 |
| 8. | Design of Test Programme | 31 |
| 8.1 | Aims | 31 |
| 8.2 | Investigation of parameters | 31 |
| 8.2.1 | Scale Effects | 31 |
| 8.2.2 | Timescale | 31 |
| 8.2.3 | Wave height, period and depth | 32 |
| 8.2.4 | Initial conditions: Bed slope | 32 |
| 8.2.5 | Initial conditions: Chronology | 33 |
| 8.2.6 | Overtopping | 33 |
| 8.2.7 | Seawall type | 34 |
| 8.2.8 | Toe protection | 34 |
| 9. | Outline Physical Model Test Programme | 35 |
| 9.1 | Series 1 | 35 |
| 9.2 | Series 2 | 35 |
| 9.3 | Series 3 | 35 |
| 9.4 | Series 4 | 36 |
| 9.5 | Test series 5 and 6 | 37 |
| 9.6 | Test series 7 | 37 |
| 9.7 | Discussion | 37 |
| 9.8 | Summary | 38 |
| 10. | References | 39 |

Contents continued

Tables

| | | |
|----------|---|----|
| Table 1 | Calculations of the percentage of waves causing suspended transport..... | 12 |
| Table 2 | Xie (1981) irregular wave suspended transport scour tests | 13 |
| Table 3 | Summary of Fowler (1992) irregular wave test conditions | 16 |
| Table 4 | Supertank target hydrodynamics for test ST_70..... | 20 |
| Table 5 | Supertank target hydrodynamics for test ST_80..... | 20 |
| Table 6 | Supertank target hydrodynamics for test ST_C0 | 21 |
| Table 7 | Summary of large scale experiments | 23 |
| Table 8 | Volume and mass of sand required for different beach configurations | 27 |
| Table 9 | Percent by weight passing sieve & fall velocity of Redhill 110 fine sand..... | 29 |
| Table 10 | Test Series 1 to 4..... | 36 |

Figures

| | | |
|-----------|---|----|
| Figure 1 | Flow chart of R&D process for improved scour prediction methodology and translation into engineering framework | 2 |
| Figure 2 | Dominant processes and modes of sediment transport (after Oumeraci, 1994)..... | 6 |
| Figure 3 | Re-circulating currents due to streaming under standing waves (Sumer and Fredsøe, 2000) | 10 |
| Figure 4 | Scour and deposition patterns in front of a vertical seawall for L-type (top) and N-type (bottom) sediment transport. After Xie (1981)..... | 10 |
| Figure 5 | Xie's (1981) regular wave best-fit maximum scour predictor, two irregular wave maximum scour depths and Equation 18 that fits the irregular wave data. | 14 |
| Figure 6 | Hughes and Fowler (1991) maximum scour depths with Equation 19..... | 15 |
| Figure 7 | Design relationship (Equation 21) and data from Fowler (1992) | 17 |
| Figure 8 | Fowler's (1992) data for scour depth at the seawall | 17 |
| Figure 9 | Position of Fowler's (1992) irregular wave scour data on parametric scour prediction axes | 18 |
| Figure 10 | Fowler (1992) measured scour at seawall plotted against prediction of McDougal et al. (1996)..... | 19 |
| Figure 11 | Summary of large-scale scour experiments with irregular waves on parametric scour plot axes. | 25 |
| Figure 12 | Proposed physical model bathymetry (note distorted scale)..... | 28 |
| Figure 13 | Sediment grading of Redhill 110 fine sand..... | 30 |
| Figure 14 | Series 1 to 4 with data from Fowler (1992). | 36 |

1. *Introduction*

HR Wallingford will be conducting medium scale physical model tests of scour in front of seawalls as part of the Defra funded project Understanding the Lowering of Beaches in front of Coastal Defence Structures, Phase 2 (FD1927). The work will be carried out with the assistance of the University of Southampton.

The tests will be carried out as new understanding and validation data for beach lowering methods are required using targeted laboratory data collection and fieldwork. During Phase 1 of the research (Sutherland et al., 2003) some shortcomings were identified in the presently available laboratory data for scour prediction in front of seawalls. The shortcomings of previous 2D (flume) tests can be addressed and overcome by medium scale tests in the laboratory at HR Wallingford. The aim of the flume experiments is to provide a set of physical model test results that will feed into the development of an improved scour prediction method. This will be used for scour predictions and will provide input to a probabilistic method for assessing the safety of coastal defence structures within the PAMS framework. The data will also be useful for the validation and development of numerical models. The selection of seawall profiles has been informed by interrogation of the NFCDD and an expert review of seawalls and beaches.

This Technical Note summarises the arguments made in the design of the physical model tests and in doing so draws heavily on Sutherland et al., (2003). It starts with reviews of the scaling arguments for physical model tests and of previous relevant medium to large scale experiments on scour in front of coastal defence structures. The new wave flumes at HR Wallingford are then described, to provide the limits on the experiments that can be performed. The aims of the test programme and the range of parameters that should be investigated are then described and a test programme is proposed. Whilst the main aim of the tests is to evaluate methods for scour prediction on sand beaches, the proposed test programme is not intended to be prescriptive and it will be optimised, depending on the results of the previous tests.

The target test matrix will be reviewed in light of any feedback received on this report. The design and execution of physical model laboratory tests is a key part of the R&D process outlined in Figure 1, where the present work is highlighted in light blue.

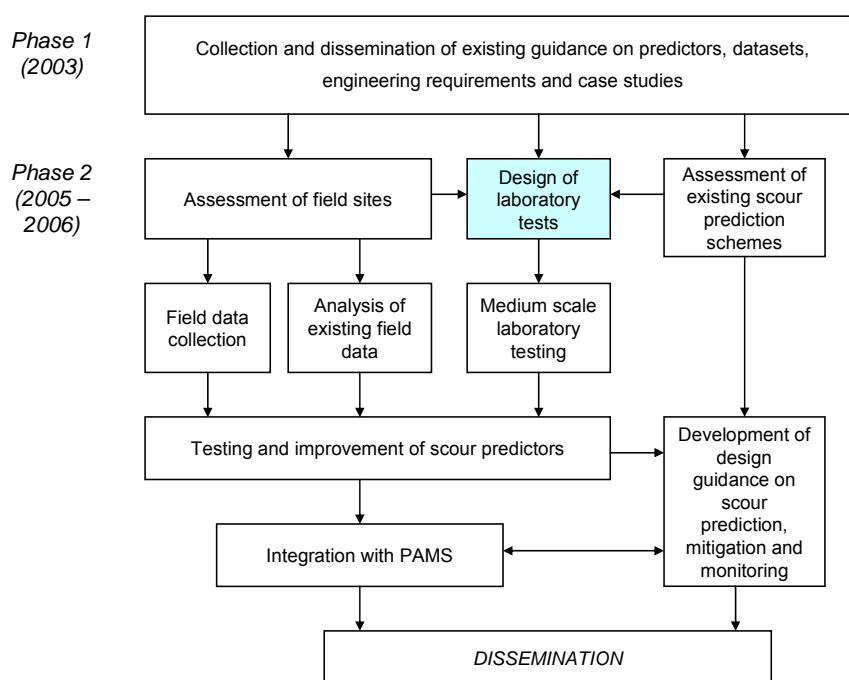


Figure 1 Flow chart of R&D process for improved scour prediction methodology and translation into engineering framework

The laboratory tests will look at the longshore-uniform case of normal wave incidence only. The field tests will look at the 3D problem (Sutherland and Pearce, 2005). In some cases both cross-shore and long-shore transport will need to be considered. To extend the laboratory tests to 3D would have meant additional time and costs for construction and running of the tests, plus additional time for analysis. Such tests could be performed at a later date as part of another study, if required.

A Technical Report will be published on the laboratory procedures and results (Project Milestone 06/01). The measurements will be analysed, interpreted and written up and will extend the existing datasets to provide more appropriate data for the validation and extension of the existing predictive methods.

2. *Interrogation of NFCDD*

The 2005 National Flood and Coastal Defence Database (NFCDD) was interrogated to identify the relative number of different critical structure types for coastal (as opposed to fluvial) flooding. The purpose of the interrogation was to provide data with which to identify the relative prevalence of different coastal defence types. The results from such a survey would indicate the importance of testing for scour in front of different structure types. The numbers of selected different structure types are shown in the following list:

Although the NFCDD does not list combinations of structure and beach, the list includes 188 seawalls, 162 breakwaters and 2276 walls, some of which are likely to be vertical or near vertical seawalls fronted by a sand beach. The seawall type behind the groyne fields (if any) is not specified. To put the numbers in context, the full list includes 2150 ‘faces’ and 1100 ‘none’s and ‘others’, so there are a lot of cases where the NFCDD does not provide enough information to determine whether there is a seawall and a beach or not. The interrogation of the NFCDD did not produce sufficient information of the right type to identify the relative prevalence of different coastal defence types fronted by sand beaches. The choice of representative structure type was therefore made by identifying which type would give the worst scour, providing there were examples of this type around the English and Welsh coastline.

In addition, a non-exhaustive expert review from site visit experience of the occurrence of (near)vertical seawalls fronted by sand beaches in England and Wales produced the following list: Berwick (south of river), Newbiggin town frontage, Blyth south beach, Whitley Bay, Roker, Seaham (some pebbles), Sandsend Whitby Sands (north of pier), Scarborough North Bay, Filey, Lowestoft at Children’s Corner, Bridlington south of harbour, Hornsea (some pebbles), Withernsea, Cleethorpes south of pier, Overstrand (some pebbles), Mundesley (some pebbles), Walton, Eastwater Bay near Dover, Ryde north and south of pier, Sandown near the zoo, Southbourne (in places), Poole (at Canford Cliffs, Shore Road and Haven Hotel), Swanage (near the Grand and the pier), Weymouth south beach, Dawlish to Teignmouth along BR line (some pebbles), Torquay, Goodrington, Marazion, Perranporth, Newquay, Weston-Super-Mare north end, Afon Wen, Nefyn, Colwyn Bay west of pier, Hoylake, New Brighton and Blackpool - Fleetwood. Photographs of many of these seawalls obtained from site visits, can be provided, if required to show the beach/wall characteristics. This list justifies the use of a vertical seawall in laboratory tests.

The expert review and the interrogation of the NFCDD have demonstrated that the provenance of seawalls and beaches is a combination with practical engineering relevance.

3. Physical Model Scaling for Scour Tests

A very thorough discussion of scale factors in various types of hydrodynamic models, both with and without sediment can be found in Hughes (1993). The discussion below is taken from Sutherland (1999) which was derived from Sutherland and Whitehouse (1998) which in turn relied on the work of Kamphuis (1985). A brief summary of some of the main parameters is given below.

It is assumed throughout that waves are scaled by the Froude number:

$$F_r = \frac{U^2}{gL} \quad (1)$$

where U is a velocity, g is gravitational acceleration and L is a length. To maintain similitude, which is required to convert model scale results to full (prototype) scale, this number must be the same in the model and prototype. The five main non-dimensional numbers for sediment transport similitude between prototype and model are listed below.

The Grain Reynolds Number:
$$R_{e*} = \frac{u_* d}{\nu} \quad (2)$$

where u_* is the shear velocity, d the (median) grain diameter and ν the fluid viscosity. The shear velocity is derived from the wave skin friction shear stress, τ_w and the water density, ρ , as $u_* = (\tau_w/\rho)^{0.5}$. The wave skin friction, or grain shear stress is that applied to a grain, rather than the total stress applied to a ripple and is used to represent the mobilising force due to the waves. The wave skin friction shear stress, the bed shear stress, τ_w , is given by $\tau_w = \frac{1}{2} \rho f_w U_w^2$ with f_w the wave friction factor and U_w the bottom orbital velocity of the wave spectrum. The wave friction factor is a function of the wave Reynolds Number, $R_w = U_w A / \nu$ with $A = U_w T / (2\pi)$ and the relative roughness, $r = A / k_s$ with k_s the Nikuradse equivalent sand grain roughness (Soulsby, 1997, Section 4.5).

The Shields Parameter:
$$\theta = \frac{\tau}{g(\rho_s - \rho)d} \quad (3)$$

where ρ_s is the density of the sediment and the other parameters are as defined above. The Shields parameter relates the mobilising forcing applied to a grain on the bed to the restoring force due to gravity. The Shields parameter can be used to determine sediment mobility:

- if $\theta < \theta_{cr}$ (where θ_{cr} is the critical Shields parameter) then the bed is immobile
- if $\theta_{cr} < \theta < 0.8$ (roughly) then the bed is mobile and rippled
- if $\theta > 0.8$ then the bed is mobile and flat with sheet flow.

Detailed discussions and practical guidance on calculating Shields parameters and bed shear stresses in waves and currents can be found in Soulsby (1997). Calculations can be made using the accompanying software SandCalc.

Relative density (or specific gravity):
$$s = \frac{\rho_s}{\rho} \quad (4)$$

Relative length:
$$l_s = \frac{l}{d} \quad (5)$$

where l is a characteristic length of the system. Kamphuis (1985) gives some guidance as to which length should be used in different experiments.

Relative fall speed

The relative fall speed can be chosen in a number of different ways. If the model is to be bedload dominant, so sediment mobility is dominated by shear stress applied at the bed, then the relative fall speed can be defined as:

$$\frac{u_*}{w_s} \tag{6a}$$

as commonly used in river sediment transport studies. Here w_s is the sediment fall speed, which can be determined from the equation in Soulsby (1997), reproduced here as Equation 11. If the ratio is greater than 1 then the sediment is often taken to be in suspension. If the model is to be dominated by suspended sediment transport the Dean fall speed parameter, D_{ws} , is commonly used:

$$D_{ws} = \frac{H_s}{w_s T_p} \tag{6b}$$

where H_s is the significant wave height, so H_s/w_s represents the time taken for a particle to fall in still water by a distance equivalent to the significant wave height.

All five of the above numbers (equations 2, 3, 4, 5 and 6a or 6b) should be the same in model and prototype if similitude is to be guaranteed. Unfortunately that is impossible to achieve except at a scale of 1:1 so compromises must be made. The most important numbers must be preserved, and the similitude between the values of others must be relaxed. In order to make an informed choice about which scale factors to preserve and which to relax, the hydrodynamics of a situation and the sediment response to the hydrodynamics must be known and the relative dominance of different mechanisms estimated.

3.1 BEDLOAD OR SUSPENDED LOAD?

A conceptual sketch of the relative importance of different modes of sediment transport has been developed by Oumeraci (1994) for natural beaches, as shown in Figure 2. Relationships to determine which mode of sediment transport dominates for scour tests are given below.

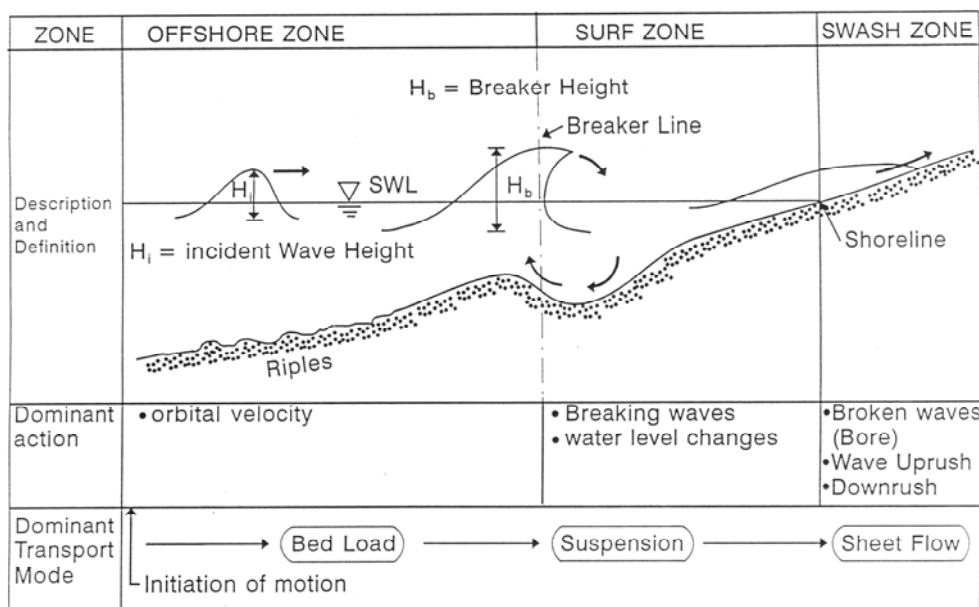


Figure 2 Dominant processes and modes of sediment transport (after Oumeraci, 1994).

Various formulae have been derived that distinguish between suspended and bedload hydrodynamic regimes. Sumer (1986) gives a criterion for currents: suspension will be initiated when the Shields parameter is greater than the threshold value, expressed as a function of dU_{fm}/ν , where d is the grain diameter, U_{fm} is the maximum value of the friction velocity and ν is the kinematic viscosity of the water. Sediment will not remain in suspension unless $U_{fm}/w_s > 1$, where w_s is the fall velocity of the sediment. This has already been given as Equation 6a.

Xie (1991) proposed the following criterion for the initiation of suspension under waves:

$$\frac{U_w - U_{cr}}{w_s} \geq 16.5, \quad (7)$$

Where U_w is the maximum value of orbital velocity at the bed and U_{cr} is the critical velocity for incipient sediment transport. Irie and Nadaoka (1984) argued that in most practical (i.e. field) cases U_m is much greater than U_{cr} , so Xie's criterion could be simplified to:

$$\frac{U_m}{w_s} \geq 10 \quad (8)$$

Note, however, that equation 7 should be used for laboratory tests, as U_m may not be much greater than U_{cr} and can be smaller than it.

Kraus and McDougal (1996) list the consequences that incorrect scaling may have:

1. Dominance of threshold of motion in the laboratory, which could alter the direction and magnitude of bed load sediment transport;
2. Presence of ripples in laboratory surf zones, which do not exist in the field and which can obscure trends in profile change;
3. Differences in sediment transport mode as suspended load or bedload between the laboratory and field;
4. Inability to scale simultaneously both bedload and suspended load, which may be particularly troublesome for experiments involving both cross-shore and long-shore transport, and different Reynolds numbers and turbulence intensity which in turn affect sediment transport mode and magnitude.

Van der Meer and Veldman (1992) conducted a berm breakwater physical model study at a scale of 1:35 and at the Deltaflume at a scale of 1:7. The depth of the scour hole produced at the toe of the structure when comparing average profiles before the highest waves hit the structure was the same in both cases, but its shape was completely different in the seaward direction. However, when comparing final profiles, the scour hole for the 1:35 test was deeper, indicating that scale effects were present in the development of the scour hole. Moreover, the authors acknowledged that these scale effects might have caused the difference in behaviour of the breakwater crest and rear face damage. Alternatively the changes in breakwater crest and rear might have caused the differences in the scour.

This supports the contention that the results from small-scale physical model results are likely to be misleading unless the most important scaling parameters are satisfied and even then should be considered as providing qualitative information. Kraus and McDougal (1996) recommended future laboratory studies to be done with justification of the scale used and with awareness of the ambiguities that have arisen in previous experiments done at small-scale. As a minimum it is recommended that the dominant transport mode (bedload or suspended) is reproduced in the laboratory. In many cases when considering sand beaches this will require suspended sediment

transport to be produced in the laboratory for a significant proportion of the time. This will require experiments to be performed at a relatively large scale.

3.2 BEDLOAD TRANSPORT SCALE MODELS

Kamphuis (1985) developed four scaling models for the bedload transport case. They are discussed in Hughes (1993) and short comments outlining the disadvantages of each may be found in Oumeraci (1994). The scaling models are:

1. Best model, which preserves the Shields parameter, the relative density and the relative length scale;
2. Lightweight model, which preserves the grain Reynolds number and the Shields parameter and uses lightweight sediment in the model, thereby preserving the relative density within a factor of 2 or so;
3. Densimetric Froude model, which preserves the Shields parameter and uses a lightweight sediment, thereby preserving the relative density within a factor of 2 or so;
4. Sand model, which preserves the relative density.

All the models have their advantages and disadvantages and the inevitable scale effects. Alternative scaling criteria will apply if the test concerns a permeable beach or structure. Yalin (1963) proposed a method for the selection of model sediment to predict the scouring of a shingle beach in front of a vertical wall using a physical model. The method used the following criteria for model scaling:

The relative magnitudes of the onshore and offshore motion should be the same in model and prototype. This can be achieved based on similarity of Dean fall speed parameter.

The threshold of motion should be correctly scaled by maintaining the same ratio of drag forces and submerged weight in model and prototype.

The permeability of the beach should be correctly reproduced by ensuring that the percolation slope of the model and prototype are the same.

The first indicates whether the beach will erode or accrete, the second determines the limiting condition for sediment transport and the third governs the beach slope in the swash zone.

Yalin's (1963) permeability criterion is that the percolation slope function should be the same in model and prototype:

$$J = k(Re_u) \frac{u^2}{gd_{10}} \quad (9)$$

With J = percolation slope, k = dimensionless permeability, a function of $Re_u = ud_{10}/\nu$ the voids Reynolds Number, with u = velocity through the voids, d_{10} = 10% undersize of the sediments and ν = kinematic viscosity. Yalin (1963) suggested that

$$\log k = 3.17 - 1.134 \log Re_u + 0.155 \log^2 Re_u \quad \text{For } 1 \leq Re_u \leq 200 \quad (10)$$

These similitude criteria formed the basis of the physical modelling of shingle beaches using lightweight sediment, coal particles, carried out by Powell and Lowe (1994). Loveless and Grant (1994) have challenged Yalin's approach, both in terms of the values of hydraulic gradient and percolation velocity assumed, and also in terms of the processes represented. A modified version of Yalin's scaling was proposed instead. If Loveless is correct, then many of the scour predictions for gravel beaches, derived from lightweight sediment models, will be

overpredictions of the actual scour. However, to test the scaling ideas out thoroughly would require a series of tests to be performed at a range of scales from almost full scale to the more typical 1:20 laboratory scale. No such test series has ever been run and so there is still uncertainty over how to scale the sediment for model tests and whether small scale model test results can be extrapolated to full scale.

3.3 SUSPENDED LOAD SCALE MODELS

Dean (1985) argued that in cases where suspended sediment is predominant the Shields parameter does not have to be preserved as the wave breaking and turbulence were more dominant mechanisms in determining sediment mobility than the wave shear stress. His recommendations were for an undistorted model with Froude scaling using the same value of the Dean fall speed parameter (Equation 6b) as in the prototype. A lightweight sediment could be used if necessary and the model should be large enough to prevent there being any effects from viscosity, surface tension or sediment particle cohesiveness. Oumeraci (1994) recommended a similar set of scaling requirements for scour tests in standing waves or under breaking waves. Hughes and Fowler (1991) also concluded that prototype conditions could be modelled if the Froude number and the Dean fall speed were preserved.

Simple Froude scaling rules exist for the fall velocities of both small and large particles (if the same density material is used in model and prototype). The fall speed of small diameter particles follows a Stokes law of viscous drag so $n_{ws} = n_L^{0.25}$ (where n_{ws} is the scale ratio of fall speeds and n_L the geometric scale ratio) as shown in Oumeraci (1994). However large particles fall by a quadratic bluff-body law (see Soulsby 1997) with fall speed proportional to the square root of the diameter. It follows that the scaling here is $n_{ws} = n_L^{0.5}$. As the scaling rule changes with the size of the sediment, and a slightly different density of water is often used in model and prototype, it is wisest to iterate to a model sediment diameter from its fall speed. Soulsby (1997, Equation 102) can be used to determine the sediment fall speed for model and prototype, w_s as:

$$w_s = \frac{\nu}{d} \left[\left(10.36^2 + 1.049 D_*^3 \right)^{1/2} - 10.36 \right] \quad (11)$$

Where D_* is the dimensionless grain size given by:

$$D_* = \left[\frac{g(s-1)}{\nu^2} \right]^{1/3} d \quad (12)$$

3.4 EFFECT OF MODE OF SEDIMENT TRANSPORT

A regular wave reflecting off a vertical wall generates a standing wave, which in turn generates steady streaming in the thin bottom boundary layer (Longuet-Higgins, 1953). This streaming is manifested as a slow recirculating current from anti-node to node at the bottom of the bottom boundary layer and from node to antinode at the top of the bottom boundary layer as shown in Figure 3 (from Sumer and Fredsøe, 2000). The current at the top of the boundary layer drives a counter-rotating re-circulating cell in the (much thicker) body of water above the boundary layer. This work was extended to oblique-incidence by Carter et al. (1973).

If the sediment in the bed is coarse and travels close to the bottom, it will be most influenced by the horizontal water movements in the bottom boundary layer, which are towards the node (the previously-named N-type, Xie, 1981). The result is scouring midway between anti-node and node and deposition under the node. If the sediment is small and is maintained in suspension, it will be most influenced by the current above the bottom boundary layer, so the net movement is away from the nodes towards the antinodes (L-type).

Therefore the basic **pattern** of sediment erosion and accretion varies with the mode of sediment transport – bedload transport gives a different pattern from suspended load transport (Sumer and Fredsøe, 2002) as shown in Figure 4. It is important to reproduce suspended sediment transport in the laboratory experiments to provide results that are applicable in the field situation where sand is suspended in the water column.

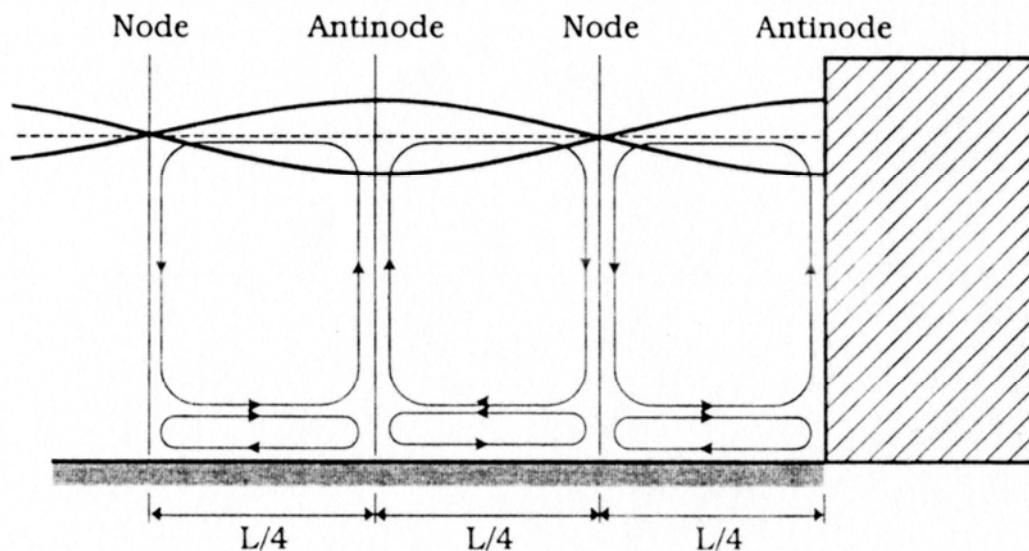


Figure 3 Re-circulating currents due to streaming under standing waves (Sumer and Fredsøe, 2000)

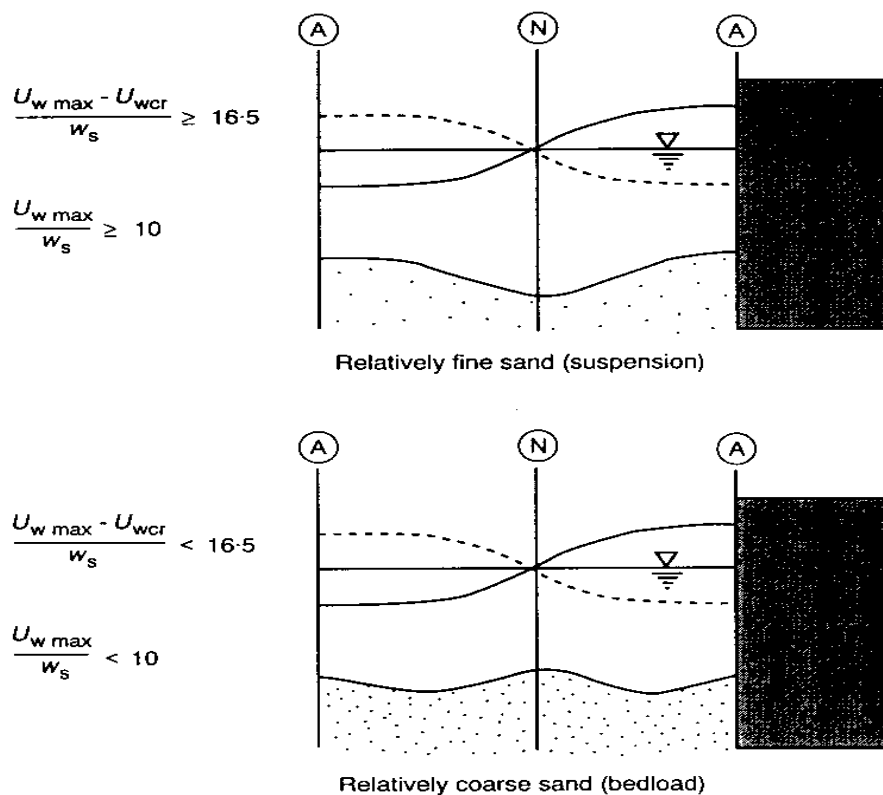


Figure 4 Scour and deposition patterns in front of a vertical seawall for L-type (top) and N-type (bottom) sediment transport. After Xie (1981).

4. Prediction of suspension

The main advantage of large scale experiments is that they are not affected by similitude problems to the same extent as smaller laboratory experiments. They are generally carried out in large scale wave flumes where suspended sediment transport can be generated. The difference between large scale and small scale experiments is taken to be that small scale experiments are usually determined by bedload sediment transport, while large scale experiments have a significant percentage of suspended sediment transport.

The equations presented below can be used as a first approximation to obtain the percentage of waves that will generate suspended sediment transport. A more detailed approach can be found in Tørum et al. (2003).

The Xie (1981) criteria for suspended sediment transport to occur is given in Equation 7. This can be re-arranged to give the minimum bed velocity required for suspension, U_{ms} , as:

$$U_{ms} = 16.5w_s + U_{cr} \quad (13)$$

The theory of Komar and Miller (1974) can be used to determine the critical velocity for incipient transport, U_{cr} as:

$$U_{cr} = [0.118g(s-1)]^{2/3} d^{1/3} T^{1/3} \quad (\text{for } d < 0.5\text{mm}). \quad (14)$$

Moreover, w_s is given by Equation 11, so U_{ms} can be determined from Equation 13, using Equations 11 and 14, given median sediment diameter, density of sediment particles and water, kinematic viscosity, wave height, wave period and water depth. The minimum wave height for suspension, H_{sus} then follows from linear theory (with the calculations simplified by assuming shallow water). Assuming a Rayleigh distribution for wave heights gives the probability that any wave is lower than or equal to a height H as:

$$P(H) = 1 - \exp\left\{-H^2/H_{rms}^2\right\} \quad (15)$$

with $H_{rms} = H_s/\sqrt{2}$ is the root mean square wave height and H_s is the significant wave height. The probability that an incident wave will not cause suspended sediment transport, $P(H_{sus})$ can then be estimated (using equation 15 and ignoring the dependence of suspension on wave period). The percentage of incident waves that will cause suspended sediment transport, is given in Equation 16:

$$\%sus = 100[1 - P(H_{sus})] \quad (16)$$

Some example calculations for non-breaking waves and a beach slope of 1:30 are given in Table 1 for a sediment diameter, $d = 0.11\text{mm}$ (fine sand). Fresh water at 10° C was assumed. The sediment fall speed, $w_s = 0.0075\text{m/s}$ for a particle density of $\rho_s = 2650\text{kg/m}^3$. Calculations based on possible experimental conditions are given in Table 1. Here the incident significant wave height, H_s , is Owen's (1980) maximum non-breaking value for the given water depth, wave period and beach slope, assuming no reflections.

The highest possible non-breaking incident significant wave heights at a depth of 0.2m will cause suspension under 56% to 62% of all waves, with peak spectral periods between 1.46s and 4.58s. Doubling the water depth would increase the percentage of waves with suspension to

between 72% and 78%. Note that these percentages are for incident waves only, with an assumed Rayleigh distribution. This will not be valid in front of a reflecting coastal structure in fairly shallow water (see for example, van Gelder and Vrijling, 2000).

Reflections caused by a seawall will increase the significant wave height, velocities and turbulence levels, all of which will increase the amount of sand in suspension. Perfect reflection would increase H_s by a factor of $\sqrt{2}$ and increasing the significant wave height by a factor of $\sqrt{2}$ for a depth of 0.2m increases the percentage of wave causing suspension to between 75% and 79%.

Producing incident waves of around $H_s = 0.2\text{m}$, for example, would cause wave breaking in front of the seawall, which would increase turbulence levels which will increase the percentage of waves producing suspended sediment transport, providing that the turbulence reaches the bed. However, Barnes et al. (1996) and Pedersen et al. (1998) have shown that the influence of spilling breakers is confined to a thin layer near the water surface, so may not influence the bed significantly. Combining wave breaking with reflection should, however, lead to a large majority of waves causing suspended sediment transport. This should make any scour predictions produced applicable to field cases with sediment in suspension.

Table 1 Calculations of the percentage of waves causing suspended transport

| Depth | H_s (m) | T_p (s) | U_{cr} (m/s) | U_{mc} (m/s) | H_c (m) | $P(H_c)$ | %sus |
|-------|-----------|-----------|-------------------|----------------|-----------|----------|------|
| 0.2 | 0.144 | 4.58 | 0.123 | 0.248 | 0.071 | 0.38 | 62% |
| 0.2 | 0.142 | 4.00 | 0.118 | 0.242 | 0.069 | 0.38 | 62% |
| 0.2 | 0.138 | 3.24 | 0.110 | 0.234 | 0.067 | 0.37 | 63% |
| 0.2 | 0.128 | 2.29 | 0.098 | 0.222 | 0.063 | 0.39 | 61% |
| 0.2 | 0.120 | 1.87 | 0.091 | 0.216 | 0.062 | 0.41 | 59% |
| 0.2 | 0.111 | 1.46 | 0.084 | 0.209 | 0.060 | 0.44 | 56% |
| 0.4 | 0.276 | 4.58 | 0.123 | 0.248 | 0.100 | 0.23 | 77% |
| 0.4 | 0.270 | 4.00 | 0.118 | 0.242 | 0.098 | 0.23 | 77% |
| 0.4 | 0.257 | 3.24 | 0.110 | 0.234 | 0.095 | 0.24 | 76% |
| 0.4 | 0.229 | 2.29 | 0.098 | 0.222 | 0.090 | 0.27 | 73% |
| 0.4 | 0.216 | 1.87 | 0.091 | 0.216 | 0.087 | 0.28 | 72% |
| 0.4 | 0.237 | 1.46 | 0.084 | 0.209 | 0.084 | 0.22 | 78% |

5. Previous suspended sediment transport physical model tests

The limited numbers of scour tests where suspended sediment transport played a large role are listed below.

5.1 XIE (1981)

Xie (1981) included a number of tests that generated scour in a flat bed in front of a vertical seawall that were in the suspension mode. Most of the tests used regular waves but three irregular wave tests were also conducted in suspension mode. Xie formulated an equation for the maximum scour depth over a flat bed for suspended sediment transport generated by regular waves, given in Equation 17:

$$\frac{S_{\max}}{H} = \frac{0.4}{(\sinh kh)^{1.35}} \quad (17)$$

Where S_{\max} is the maximum scour depth, H is the regular wave height, $k=2\pi/L$ is the wavenumber (with L the wavelength) and h is the initial water depth at the toe of the seawall. Although three irregular wave tests were conducted, only two maximum scour depths are quoted as the middle test (2c) was terminated early. Details of the three tests are given in Table 2 and the results are plotted with Equation 17 in Figure 5, where H_s has been used in place of H and the wavenumber has been calculated at the spectral peak wave period. Note that the maximum scour depth was at the first partial node in front of the breakwater, not at the breakwater toe, where accretion occurred (as illustrated in the top panel of Figure 4). The two irregular wave results suggest that the maximum scour depth could be predicted by a formula similar to Equation 17, but with a lower numerator and / or a different power in the denominator. Fitting an equation with the form of Equation 17 to the two data points gives Equation 18, which is also shown in Figure 5 but which should not be used for design as there are so few data points.

$$\frac{S_{\max}}{H_s} = \frac{0.34}{(\sinh k_p h)^{0.81}} \quad (18)$$

Xie's tests were conducted on a flat sand bed in relatively deep water ($h_t / H_s > 4$) so there can have been few breaking waves and little turbulence reaching the bed. The sediment transport was dominated by streaming in the convection cells set up in front of the seawall. The pattern of decaying accretion and scour starts with accretion at the seawall. Therefore the scour depth at the seawall, S_t , was negative in both cases, as shown in Table 2.

Table 2 Xie (1981) irregular wave suspended transport scour tests

| Test | d_{50} [mm] | h [m] | H_s [m] | T_p [s] | L [m] | S_{\max} [m] | S_t [m] |
|------|------------------|---------|-----------|-----------|---------|-------------------|-----------|
| 1c | 0.106 | 0.5 | 0.085 | 1.72 | 3.37 | 0.027 | -0.029 |
| 2c | 0.106 | 0.5 | 0.091 | 1.98 | 4 | - | - |
| 3c | 0.106 | 0.3 | 0.071 | 1.69 | 2.7 | 0.03 | -0.039 |

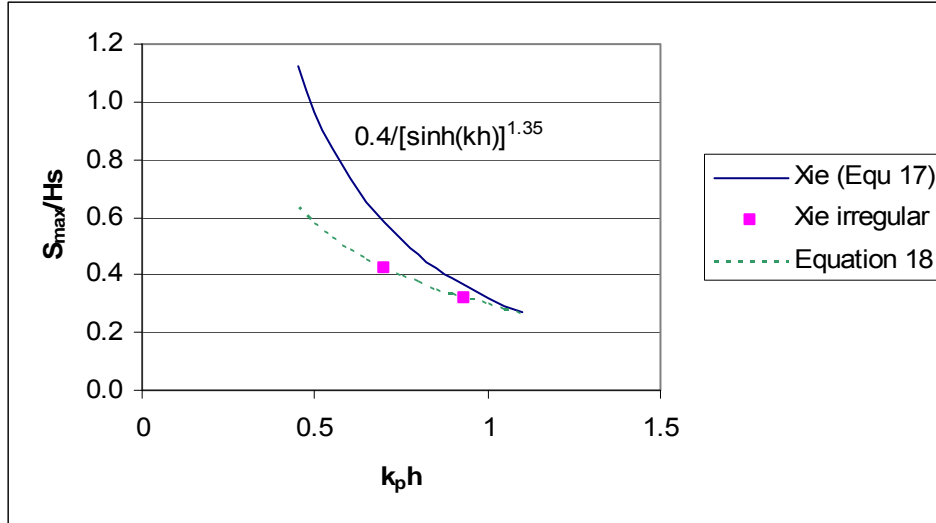


Figure 5 Xie's (1981) regular wave best-fit maximum scour predictor, two irregular wave maximum scour depths and Equation 18 that fits the irregular wave data.

5.2 HUGHES & FOWLER (1991)

Hughes and Fowler (1991) derived a modified version of Xie's formula for normally-incident, nonbreaking, irregular waves reflected by a vertical wall on a flat bottom, shown in Equation 19.

$$\frac{S_{max}}{T_p (u_{rms})_m} = \frac{0.05}{[\sinh(k_p h)]^{0.35}} \quad (19)$$

Where

S_{max} = maximum scour depth at the node (a distance $L/4$ from the wall with L the wavelength);

T_p = spectral peak wave period;

k_p = incident wavenumber (at the spectral peak);

h = water depth;

$(u_{rms})_m$ = maximum root-mean-square velocity at the bottom, which can be calculated by linear theory, given incident wave conditions and reflection coefficient or by Equation 20:

$$\frac{(u_{rms})_m}{gk_p T_p H_{m0}} = \frac{\sqrt{2}}{4\pi \cosh(k_p h)} \left[0.54 \cosh\left(\frac{1.5 - k_p h}{2.8}\right) \right] \quad (20)$$

which is valid in the range $0.05 < k_p h < 3$.

The results were calibrated using four physical model tests. In each case there was a negative correlation between the variation of rms velocity with distance in front of the structure and scour depth in front of the structure of the form $S(x) = -a \times u_{rms}(x) + b$ with (x) denoting a function of x , the distance from the seawall toe and a and b fitted coefficients. The maximum scour depth, S_{max} , occurred at the first node (approximately $L_p/4$ from the seawall) and accretion occurred at the seawall toe for test 2 (the only profile shown). Equation 19 is a fit of the maximum scour depths measured to Xie's form of equation, as shown in Figure 6. Unfortunately the wave and seabed parameters were not presented individually to allow the calculation of alternative design relationships.

The maximum scour depth measured was substantially smaller under irregular waves than under regular waves. The authors concluded that toe scour may not be of significance for design and that prediction methods for the majority of the scour problems experienced at coastal structures are still lacking.

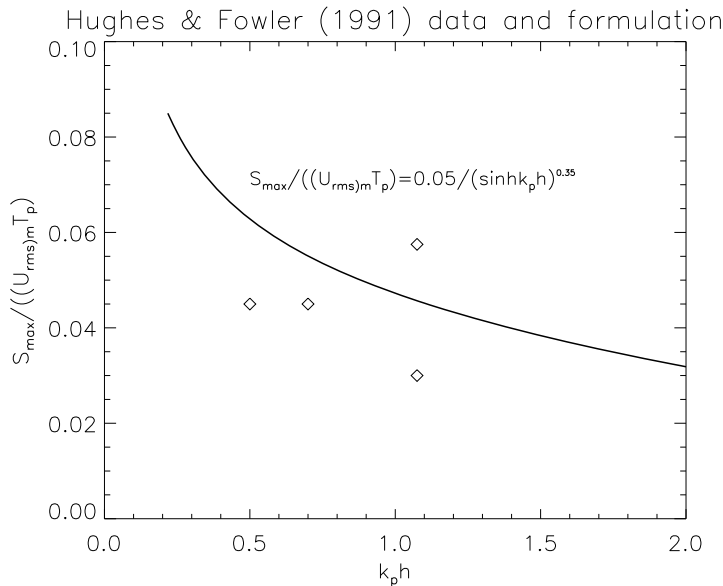


Figure 6 Hughes and Fowler (1991) maximum scour depths with Equation 19

5.3 FOWLER (1992)

Fowler (1992) performed mid-scale (wave heights between 0.2 and 0.3m) laboratory tests of the scouring of a 1:15 sloping sand bed in front of a vertical wall. Fowler used a scaling law to preserve the similitude of the dimensionless fall speed number between model and prototype. Results from the tests were compared with those from several previous laboratory studies and an empirical equation for scour prediction was developed in which the ratio of the depth of water at the wall to the deep-water wavelength was the important parameter.

Fowler's (1992) tests were valid for:

- Breaking waves
- Normally incident
- Vertical walls
- Beach in front of structure
- Sand

Tests were performed within the following limits of applicability:

- $-0.011 < h_t / L_0 < 0.045$ and
- $0.015 < H_s / L_0 < 0.040$

Where h_t = water depth at the seawall, L_0 = deep water linear theory wavelength, H_s = deepwater linear theory spectral significant wave height.

A total of 18 irregular wave tests and four regular wave tests were conducted in a 100m long wave flume. Each test started with a planar beach at a slope of $m=1:15$. A vertical seawall was used for all tests, at a cross-shore location of $x_w=0.9, 0$ and $-0.9m$ where $x_w = 0$ at the

intersection of the beach and still water level and x_w increases on moving offshore. Ottawa sand, with $d_{50}=0.13\text{mm}$ and a specific gravity of 2.65 was used in all cases. Fowler (1992) used a value of $g = 9.844\text{m/s}^2$ for gravitational acceleration and quoted a sediment fall speed, $w_s = 1.64\text{cm/s}$ (Fowler, 1992, p19) and $w_s = 1.92\text{cm/s}$ (Fowler, 1992, Table 1, using 1foot = 0.3048m). A water temperature of 25°C was used by him in all calculations. Waves were run for bursts of 300s, but as many bursts as needed to reach equilibrium were run for an experiment.

The irregular wave test conditions are shown in Table 3. Here, the maximum scour depth S_{max} is the maximum final bed elevation below the initial profile at cross-shore position X_{max} (metres offshore from seawall). The maximum erosion depth at the seawall is denoted S_t .

Equation 21 shows Fowler’s design relationship for maximum scour depth, S_{max} . Equation 21 is plotted with Fowler’s irregular wave data in Figure 7. The non-dimensional ratio S_{max}/H_s from Fowler (1992, Table 1 column 11) is plotted as “From report” while the same ratio recalculated from Fowler (1992, Table 1, columns 4 and 8) is plotted as “Fowler 1992 recalculated” as there are some inconsistencies between the two versions of the same ratio. The recalculated ratios, based on quoted H_s and S_{max} values will be used henceforth.

$$\frac{S_{max}}{H_s} = \left(22.72 \frac{h_t}{L_0} + 0.25 \right)^{1/2} \quad (21)$$

Table 3 Summary of Fowler (1992) irregular wave test conditions

| Test | x_w (m) | h_t (m) | H_s (m) | T_0 (s) | L_0 (m) | S_{max} (m) | X_{max} (m) | S_t (m) | $\frac{S_{max}}{H_s}$ | $\frac{S_t}{H_s}$ |
|------|-----------|-----------|-----------|-----------|-----------|---------------|---------------|-----------|-----------------------|-------------------|
| S1 | 0 | 0.061 | 0.211 | 1.97 | 6.081 | -0.134 | 0.000 | -0.134 | 0.63 | 0.63 |
| S2 | 0 | 0.000 | 0.201 | 1.97 | 6.081 | -0.082 | 0.000 | -0.082 | 0.41 | 0.41 |
| S3 | 0 | 0.061 | 0.208 | 1.97 | 6.081 | -0.152 | 0.000 | -0.152 | 0.73 | 0.73 |
| S4 | 0 | 0.061 | 0.239 | 2.49 | 9.714 | -0.192 | 0.000 | -0.192 | 0.80 | 0.80 |
| S5 | 0 | -0.030 | 0.257 | 1.97 | 6.081 | -0.064 | 1.524 | -0.024 | 0.25 | 0.09 |
| S6 | 0 | -0.030 | 0.270 | 2.45 | 9.403 | -0.082 | 0.305 | -0.079 | 0.30 | 0.29 |
| S7 | 0 | -0.030 | 0.244 | 1.97 | 6.081 | -0.082 | 0.305 | -0.067 | 0.34 | 0.28 |
| S8 | 0 | 0.061 | 0.195 | 1.97 | 6.081 | -0.177 | 0.000 | -0.177 | 0.90 | 0.90 |
| S9 | 0.914 | 0.061 | 0.300 | 2.43 | 9.251 | -0.122 | 0.000 | -0.122 | 0.41 | 0.41 |
| S10 | 0.914 | 0.061 | 0.208 | 1.93 | 5.837 | -0.155 | 0.000 | -0.155 | 0.75 | 0.75 |
| S11 | 0.914 | 0.030 | 0.213 | 1.97 | 6.081 | -0.143 | 0.000 | -0.143 | 0.67 | 0.67 |
| S12 | 0.914 | 0.122 | 0.208 | 1.99 | 6.203 | -0.125 | 0.000 | -0.125 | 0.60 | 0.60 |
| S13 | 0.914 | 0.122 | 0.273 | 2.4 | 9.025 | -0.213 | 0.000 | -0.213 | 0.78 | 0.78 |
| S14 | 0.914 | 0.030 | 0.290 | 2.45 | 9.403 | -0.186 | 0.000 | -0.186 | 0.64 | 0.64 |
| S15 | -0.914 | -0.061 | 0.269 | 2.45 | 9.403 | -0.073 | 0.610 | -0.034 | 0.27 | 0.12 |
| S16 | -0.914 | -0.061 | 0.200 | 1.97 | 6.081 | -0.043 | 1.524 | 0.009 | 0.21 | -0.05 |
| S17 | -0.914 | -0.091 | 0.267 | 2.48 | 9.635 | -0.052 | 1.067 | 0.027 | 0.19 | -0.10 |
| S18 | -0.914 | 0.000 | 0.201 | 1.95 | 5.956 | -0.085 | 1.219 | 0.005 | 0.42 | -0.02 |

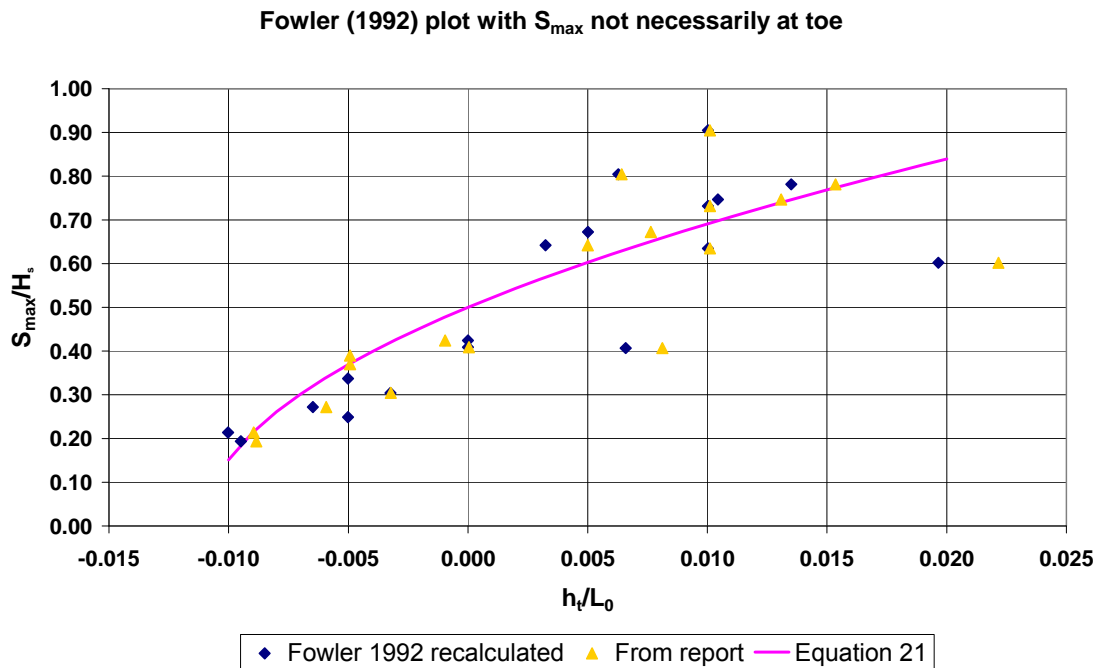


Figure 7 Design relationship (Equation 21) and data from Fowler (1992)

Note that in Table 3 the maximum scour depth is not always at the breakwater toe. The non-dimensional scour depth at the toe of the breakwater is plotted against h_t/L_0 in Figure 8. This shows a different variation of scour with relative depth and includes some negative values (i.e. accretion).

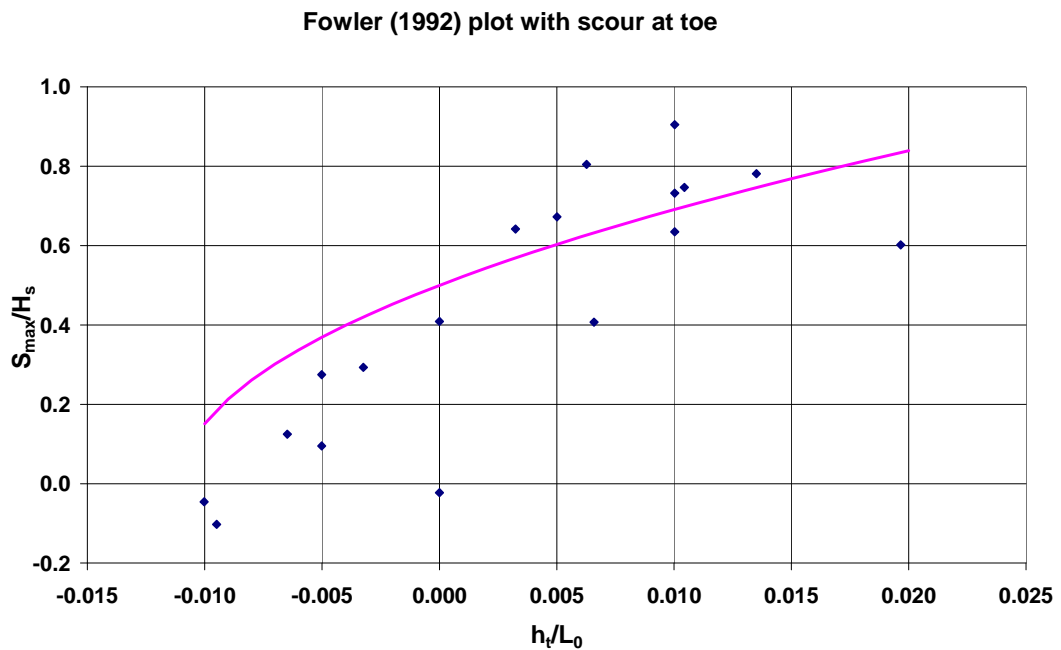


Figure 8 Fowler's (1992) data for scour depth at the seawall

Figure 9 shows Fowler's (1992) scour data plotted on the axes of a Powell and Whitehouse parametric scour plot. The numbers beside the data point are the values of S_t/H_s where S_t is the scour depth at the seawall and H_s is the deep water incident significant wave height. The results are broadly consistent with high values to the top left of the plot and lower values to the right and negative values (accretion) towards the bottom. There are some areas where nearby S_t/H_s values show considerable differences (0.91 and 0.41, for example or 0.41 and -0.02).

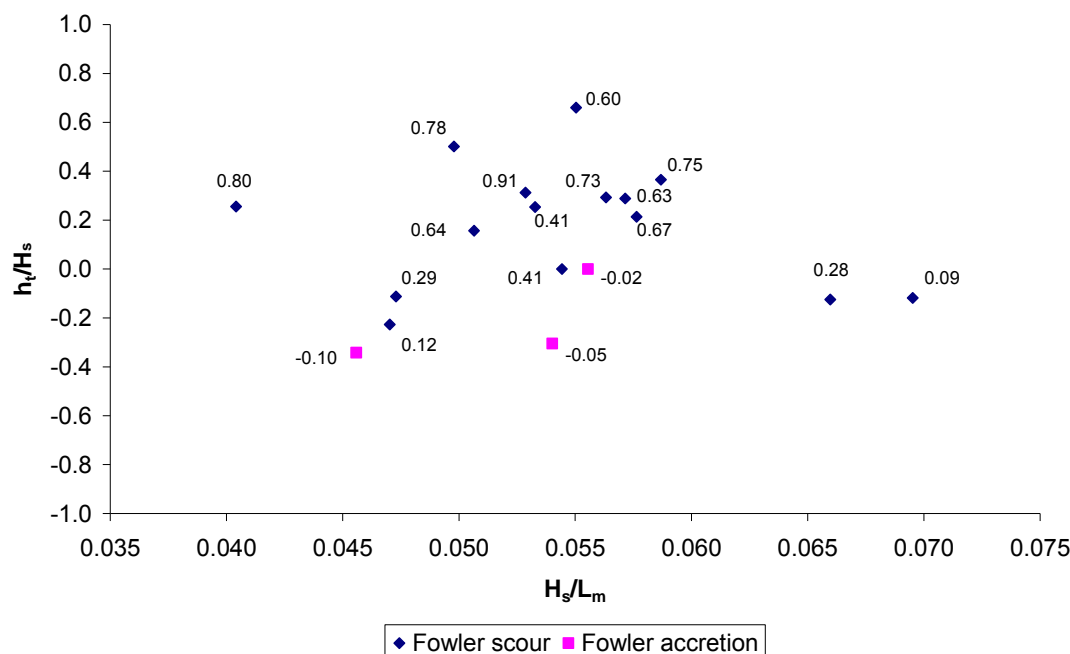


Figure 9 Position of Fowler's (1992) irregular wave scour data on parametric scour prediction axes

Fowler also compared Equation 21 to data from the regular wave experiments of Barnett (1989) and Chesnutt and Schiller (1971) – where H_0 was taken as the wave height from the regular tests. Although there was large scatter, they followed the same trend. Only irregular wave data is considered here, so that comparison is not included.

5.3.1 Drawbacks

In a review of scour processes, McDougal et al. (1996) identified that the equation proposed by Fowler includes an inverse dependency between the dimensionless scour depth and the deepwater wavelength, or wave period. As a result, Fowler's equation implies that the dimensionless scour increases with increasing wave steepness; a result which runs contrary to other scour prediction equations. Moreover, Kraus and McDougal (1996) considered that the planar initial slope of 1 in 15 was not in equilibrium under surf zone waves, which may have exaggerated the scour produced.

Figure 10 shows Fowler's (1992) measured non-dimensional scour depth plotted against Equation 20 of McDougal et al. (1996) which is determined in terms of the deep-water wave height, H_0 and is reproduced as Equation 22 here.

$$\frac{S_w}{H_0} = 0.41m^{0.85} \left(\frac{L_0}{H_0} \right)^{1/5} \left(\frac{h_t}{H_0} \right)^{1/4} \left(\frac{H_0}{d_{50}} \right)^{1/3} \quad (22)$$

The scour depth increases as the wave period and hence wavelength increases. This contrasts with Equation 21 where scour depth increases as wavelength decreases. Fowler's (1992) irregular wave data with $h_t \geq 0$ is plotted against Equation 22 in Figure 10. The predictions fit the form of the data, although the fit to the data is hardly convincing. However, increasing scour depth with increasing period fits Xie (1981) and Xie-type scour equations and Powell and Whitehouse (1998) parametric scour plot.

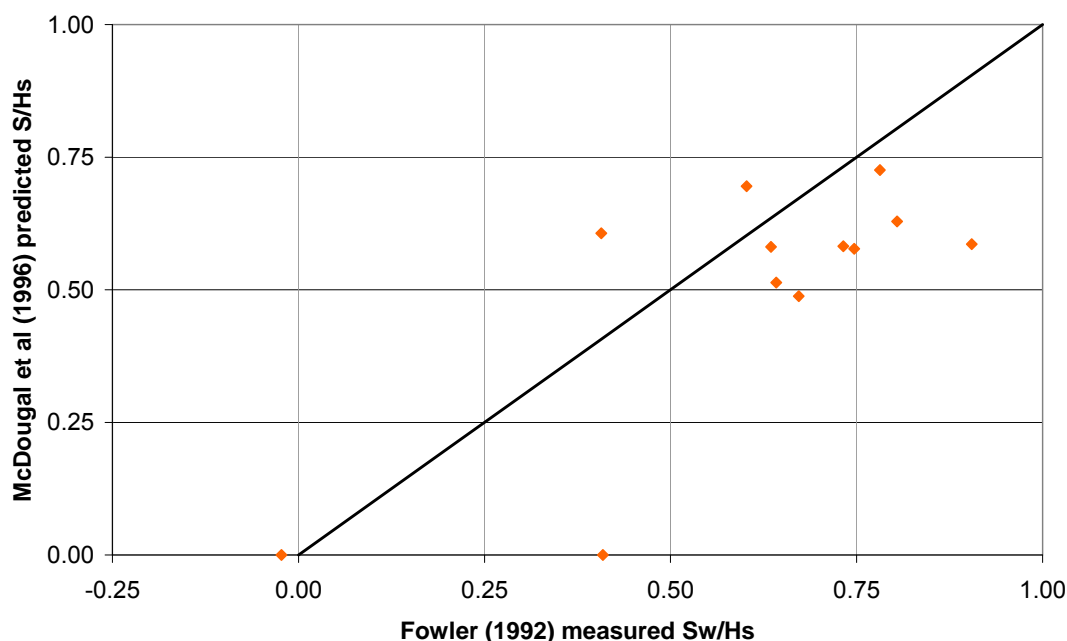


Figure 10 Fowler (1992) measured scour at seawall plotted against prediction of McDougal et al. (1996)

Fowler's (1992) irregular wave data can be used to broadly support the scour prediction approaches of Fowler (1992), McDougal et al. (1996) and Powell and Whitehouse (1998) even though they give different (sometimes opposing) dependencies on wave period. Distinguishing between them would require using statistical measures of the goodness of fit. It is worth noting that Equation 20 (Fowler 1992) was fitted to Fowler's data, so should fit it better than the other two approaches which were not.

One limitation of Fowler's data is that it occupies a limited range of relative wave steepness ($0.04 \leq H_s/L_m \leq 0.07$) and relative toe depth ($-0.35 \leq h_t/H_s \leq 0.59$). The range of steepness was intended to model the range found in erosive storms. It seems not to have been enough to determine the variation of scour depth with period. A broader range of relative depth should be modelled using a broader range of frequencies.

5.4 SUPERTANK

The SUPERTANK Data Collection Project was performed at the O.H. Hinsdale Wave Research Laboratory (WRL), Oregon State University between 29 July and 20 September 1991 (Kraus et al., 1992, Kraus and Smith, 1994). The WRL flume is 104.2m long, 3.66m wide and 4.57m (15 feet) deep. The beach was made of very well-graded sand trucked from the Oregon coast with a median diameter, $d_{50} = 0.22\text{mm}$ (determined by sieving) and a quoted fall speed of 0.033m/s. Waves with a TMA spectral shape (and $\gamma=3.3$) were generated in all cases. Three seawall scour tests were conducted with vertical seawalls:

- ST_70 had a wave condition designed to be erosive and the seawall at $x = 0.305\text{m}$;
- ST_80 had a terraced profile so waves could attack the wall more directly than in ST_70 and used the same seawall as Test ST_70;
- ST_C0 had small waves run to provide a natural profile before steep waves were run and the seawall at $x = 11.28\text{m}$.

Each test was run in a number of short stages (of 10, 20, 30, 40 or 70 minutes) with the bed profile being measured after each stage. The target hydrodynamic conditions for experiments ST_70, ST_80 and ST_C0 are shown in Table 4, Table 5 and Table 6 respectively. Beach levels at the toe and water depth at the toe were measured at the end of each test series. Water and beach levels are positive upwards, with a datum on the top wall of the flume. Negative water depths at the toe imply that the beach extended above water level. Cross-shore coordinate, x is measured from the beach end of the deep section of the flume with x increasing offshore (towards the paddle).

Table 4 Supertank target hydrodynamics for test ST_70

| ST_70 | Dur (min) | T_p (s) | H_{m0} (m) | γ | Water level (m) | Beach level at toe (m) | Water depth at toe (m) | No. T_p waves, N | Sum T_m waves | H_{m0} at WG1 (m) | T_p at WG1 (s) |
|----------------|--------------|--------------|-----------------|----------|-----------------------|---------------------------------|---------------------------------|--------------------------|-----------------------|------------------------------|------------------------|
| pre-cal survey | | | | | | -1.582 | | | | | |
| A2609A | 10 | 4.5 | 0.7 | 3.3 | -1.642 | -1.579 | -0.060 | 133.3 | | 0.264 | 5 |
| A2610A | 20 | 4.5 | 0.7 | 3.3 | -1.642 | -1.490 | -0.063 | 266.7 | | 0.277 | 4.4 |
| A2610B | 40 | 4.5 | 0.7 | 3.3 | -1.642 | -1.442 | -0.152 | 533.3 | 1195 | 0.28 | 4.3 |
| A2612B | 10 | 4.5 | 0.7 | 3.3 | -1.488 | -1.390 | -0.046 | 133.3 | | | |
| A2613A | 20 | 4.5 | 0.7 | 3.3 | -1.488 | -1.311 | -0.098 | 266.7 | | 0.345 | 4.3 |
| A2614A | 20 | 4.5 | 1 | 3.3 | -1.488 | -1.286 | -0.177 | 266.7 | | 0.363 | 4.7 |
| A2615A | 40 | 4.5 | 1 | 3.3 | -1.488 | -1.244 | -0.202 | 533.3 | 1536 | 0.369 | 4.7 |
| A2617B | 10 | 4.5 | 0.8 | 3.3 | -1.180 | -1.362 | 0.064 | 133.3 | | 0.517 | 4.7 |
| A2618A | 20 | 4.5 | 0.7 | 3.3 | -1.180 | -1.451 | 0.183 | 266.7 | | 0.506 | 4.6 |
| A2618B | 20 | 4.5 | 0.7 | 3.3 | -1.180 | -1.490 | 0.271 | 266.7 | 854 | 0.502 | 4.6 |

Table 5 Supertank target hydrodynamics for test ST_80

| ST_80 | Dur (min) | T_p (s) | H_{m0} (m) | γ | Water level (m) | Beach level at toe (m) | Water depth at toe (m) | No. T_p waves, N | Sum T_m waves | H_{m0} at WG1 (m) | T_p at WG1 (s) |
|----------------|--------------|--------------|-----------------|----------|-----------------------|---------------------------------|---------------------------------|--------------------------|-----------------------|------------------------------|------------------------|
| pre-cal survey | | | | | | -1.789 | | | | | |
| A2708A | 10 | 4.5 | 0.7 | 3.3 | -1.219 | -1.786 | 0.570 | 133.3 | | 0.483 | 4.6 |
| A2708B | 20 | 4.5 | 0.7 | 3.3 | -1.219 | -1.807 | 0.567 | 266.7 | | 0.5 | 4.7 |
| A2709A | 70 | 4.5 | 0.7 | 3.3 | -1.219 | -1.841 | 0.588 | 933.3 | 1707 | 0.494 | 4.7 |
| A2710A | 20 | 4.5 | 0.7 | MONO | -1.219 | -1.844 | 0.622 | 266.7 | | 0.48 | 4.5 |
| A2711A | 40 | 4.5 | 0.7 | MONO | -1.219 | -1.829 | 0.625 | 533.3 | 1024 | 0.474 | 4.5 |

Table 6 *Supertank target hydrodynamics for test ST_CO*

| ST_CO | Dur (min) | T _p (s) | H _{m0} (m) | γ | Water level (m) | Beach level at toe (m) | Water depth at toe (m) | No. T _p waves, N | Sum T _m waves | H _{m0} at WG1 (m) | T _p at WG1 (s) |
|------------------|--------------|-----------------------|------------------------|-----|-----------------------|---------------------------------|---------------------------------|-----------------------------------|--------------------------------|-------------------------------------|---------------------------------|
| pre-test profile | | | | | | -1.939 | | | | | |
| S0209B* | 10 | 3 | 0.8 | 3.3 | -1.829 | -1.978 | 0.110 | 200.0 | | 0.342 | 3.2 |
| S02010A | 20 | 3 | 0.8 | 3.3 | -1.829 | -2.042 | 0.149 | 400.0 | | 0.377 | 3.2 |
| S0211A | 40 | 3 | 0.8 | 3.3 | -1.829 | -2.079 | 0.213 | 800.0 | | 0.381 | 3.4 |
| S0214A | 20 | 3 | 0.8 | 3.3 | -1.829 | -2.161 | 0.250 | 400.0 | | 0.614 | 2.9 |
| S0214B | 40 | 3 | 0.8 | 3.3 | -1.829 | -2.240 | 0.332 | 800.0 | 3329 | 0.621 | 3 |
| S0216A | 40 | 3 | 0.4 | 3.3 | -1.829 | -2.231 | 0.411 | 800.0 | | 0.517 | 3 |
| S0217A | 40 | 8 | 0.4 | 3.3 | -1.829 | -2.332 | 0.402 | 300.0 | 1408 | 0.5 | 7.8 |
| S0218A | 36 | 8 | 0.7 | 3.3 | -1.829 | -2.335 | 0.503 | 270.0 | 346 | 0.643 | 8.3 |

None of the experiments was allowed to run for a long time, with the greatest number of waves being 3330 before conditions were changed. Interpreting the results is therefore a challenge as time-scale as well as scour depth should be accounted for. Note that for test ST_70, the toe of the beach appears to have been above still water level at the start of the test (i.e. negative water depth at toe in Table 4). The report leaves some doubt as to the vertical datum used for water level, but quoted “water levels” have been taken to be water depths above the flat floor of the flume at a point where the flume is 15 feet deep. Therefore a level of 9 feet is taken to be at 15 – 9 = 6 feet below the top of the flume, which is the vertical datum, from which profile elevations have been measured. The calculated levels of the beach toe are in reasonable agreement with the locations of the horizontal and vertical scale marks in Smith and Kraus (1994, Volume 2, pages B28, B30 and B34) but do not agree with the initial water depth shown in McDougal et al. (1996, Figure 4 and 6 – although Figure 5 does agree).

In all cases the total (incident plus reflected) spectral significant wave height at station 1 (the innermost gauge) was considerably lower than the offshore value. In test ST_70 the waves broke about 20m seawards of the seawall, generating a breaker bar. The beach profile was quite flat inshore of this point and dissipated wave energy before it reached the seawall. Indeed the seawall was situated above mean water level, so the seawall was only exposed to wave action when setup + runup was greater than the toe elevation, until the water level was raised for the last time. In test ST_70 the offshore target incident significant wave height was 0.70m, but the first measured total incident and reflected wave height at wave gauge 1 was 0.264m, when wave gauge 1 was at x = 18.59m, 18.29m offshore from the seawall. The measured wave height at wave gauge 1 increased significantly towards the end of the test, due to an increased water level and some erosion, which reduced the amount of wave dissipation that occurred.

The SUPERTANK tests emphasise the importance of the offshore bathymetry in the prediction of scour. Traditional smaller-scale laboratory tests have tended to use a planar sloping beach or a flat bed as the initial condition for each test. In these cases the wave conditions near the seawall are often closely related to the offshore conditions. A smooth, monotonic profile was not used at SUPERTANK due to the time and effort involved. Rather, initial profiles were either the end profile of the previous test, or a modification of it. Incident wave conditions in SUPERTANK were influenced by the presence of a sand berm in front of the seawall in tests ST_70 and ST_80, when the seawall was at cross-shore coordinate x = 0.305m. Only test ST_CO used an almost planar sloping beach, with the seawall at cross-shore coordinate x = 11.28m. In this case there was a total of 170 minutes of waves with target values of H_{m0} = 0.8m and T_p = 3s acting on a beach with a local slope of 1.26 in 30m (1:23.8) and an initial toe depth of h_t = 0.110m. This sea state caused 0.30m of erosion at the toe of the seawall. The

corresponding non-dimensional ratios are $h_i/L_0 = 0.0078$ and $S/H_{m0} = 0.375$ with H_{m0} the offshore significant wave height. Note, however, that $S/H_{local} = 0.88$, using H_{local} which is the local significant wave height measured at the inshore gauge, which was 7.32m seaward of the seawall.

5.4.1 SUPERTANK summary

The large-scale SUPERTANK Laboratory Data Collection results involving seawalls are discussed in Kraus, Smith and Sollitt (1992), Kraus and Smith (1994) and McDougal et al. (1996). The programme involved three seawall tests where wave heights and periods were selected to correspond to destructive and constructive wave conditions. A remarkable result (according to the authors) was that the profiles in front of the walls did not develop a large scour trench (nor did they erode or accrete). A small scour trench was created at the toe of the wall, but the influence was highly localised in the immediate vicinity of the wall. The limited scour found was interpreted as suggesting that the scour trench sometimes observed in the field after storms may be a result of longshore transport or combined cross-shore and longshore transport occurring at the time of the storm.

However, it should be noted that in two of the cases (ST_70 and ST_80) a relatively large and relatively flat sand berm existed in front of the structure. This significantly altered the incident wave characteristics in front of the structure and showed that the common use of offshore incident wave height in predicting scour is unlikely to be applicable in such cases. The only test that did use a monotonic, concave profile was test ST_C0. In this case noticeable scour did occur. Moreover, the predicted timescale of scour was quite long and the length of each test was relatively short, so many cases did not reach equilibrium.

Measured results from SUPERTANK were used to verify the modified (including wave reflection at vertical walls) profile response model SBEACH, in the three cases obtaining good comparisons. Comparison between the original and modified profile response model SBEACH showed numerically that the beach profiles developed with and without a seawall were similar, in agreement with Hughes and Fowler (1990) results. The magnitude and time dependency of scour in front of vertical seawalls were numerically investigated with the enhanced SBEACH model, developing Equation 22 for scour. The main difficulties with Equation 22 are that it gives zero scour depth for $h_i = 0$, will not work for negative toe depths (i.e. situations where the toe is out of the water) and has a dependency on grain size.

5.5 GWK

Experiments on dune stability with dune protection structures (consisting of sandbags) were carried out in the GWK large wave flume as part of the 1996/97 experiments for the SAFE project, as described in Dette et al. (1998, 2002). Two different heights of such protection structures were tested (no-overtopping and partial overtopping allowed) and compared to the profile development when unprotected. As the sand container barrier interrupted the seaward-directed sediment transport, no dune erosion occurred and the profile in front of the barrier was flattened, mainly due to reflections. The initial 1:20 beach slope in front of the barrier between the 4m and 5m contour line disappeared completely, the material having been moved seaward to form a bar. The main difference between the two barrier height tests was that the profile change for the partial overtopping was less pronounced as the reduced barrier allowed partial overtopping of waves by which sand from the dune behind the barrier was transported into the foreshore profile.

5.6 SAKAKIYAMA AND KAJIMA (2002)

Sakakiyama and Kajima (2002) investigated toe scouring in front of a seawall covered with armour units using large- and small-scale physical model tests. Comparison of the profile changes between both tests showed that there was no scour at the toe of the armour layer. Scour was only found under regular waves for the small-scale tests. In the large-scale tests some tetrapods settled through a gravel mat into the sand bed.

5.7 SUMMARY OF SUSPENSION MODES SCOUR TESTS

A summary of the hydrodynamic conditions of the large scale tests is provided in Table 7 and the results for scour at the seawall are shown in Figure 11.

Table 7 Summary of large scale experiments

| | H_0 offshore wave height (m) | T_p Period(s) | h_t water depth at toe (m) | Structure type | d_{50} Grain size (mm) | m Bed slope | Grain fall speed (m/s) |
|--|--------------------------------------|--------------------|------------------------------------|---|-----------------------------------|---|------------------------------|
| Xie (1981) | 0.071, 0.085 | 1.7 | 0.3, 0.5 | vertical | 0.106 | 0 | 0.0069 |
| Hughes & Fowler (1991) | NA | NA | NA | vertical | 0.13 | 0 | 0.0164 |
| Fowler (1992) | 0.2-0.29 | 1.95-2.49 | 0.06, 0, - 0.06 | vertical wall | 0.13 | 1 in 15 | 0.0164 |
| Supertank | 0.4 to 1.0 | 3.0 to 8.0 | ≈ 0.35 , 0.4, 0.6 | vertical | 0.22 | Initially at $x^{2/3}$ but for the rest of the tests using end conditions from previous tests | 0.033 |
| GWK (Dette et al., 1998) | 0.65-1.2 | 5.5 | ≈ 0 | vertical dune barriers (sandbags) | 0.3 | End position from previous test | 0.042 |
| Sakakiyama and Kajima (2002) Scale of 1/22.7 | 0.45-0.56 | 3.36 | ≈ 1.05 | Tetrapod units in front of caisson | 0.2 | 1 in 40 | |

Xie (1981) conducted two irregular wave scour tests with a vertical wall and a flat sand bed, with sediment transport in the suspended mode. Xie's tests were in relatively deep water ($h_t / H_s > 4$) so there can have been few breaking waves and little turbulence reaching the bed. The sediment transport was dominated by streaming in the convection cells set up in front of the seawall. The pattern of decaying accretion and scour starts with accretion at the seawall. Therefore the scour depth at the seawall, S_t is negative in both cases, as shown in Table 2 and Figure 11. The maximum scour depth occurred at a distance $L/4$ from the vertical wall at the first node in the partial standing wave field and followed a similar trend to Xie's result for regular waves, as shown in Figure 4, with the best-fit line given by equation 18.

The location of the scour and accretion depends on the partial standing wave pattern generated in front of the wall. This can be reasonably predicted using linear theory (O'Donoghue and Sutherland, 1999). Note that the position of the partial standing wave and hence scour and accretion will change from that above if the angle of the seawall changes, so that it is possible to have scour at the seawall toe for sloping seawalls.

Hughes and Fowler (1991) conducted a similar set of tests to Xie, although only non-dimensional quantities are quoted so values of wave height, period and depth are not available from the published sources for direct comparison. Their results exhibited a similar trend to Xie, although their fit to a Xie-type curve was poor. Xie and Hughes and Fowler's tests provide one limiting case of scour and accretion in front of coastal structures for relatively deep water and flat beds.

Hughes and Fowler (1990) conducted a single irregular wave scour test with a vertical sea wall. They used a very steep initial beach slope of 1:4, which is unrealistic for a natural beach. The scour depth was limited by the presence of a 1:4 revetment under the sand layer, which became exposed within 370 waves of the start of the test, so a value of $S_t/H_s = 1.37$ was therefore the highest scour depth that could be attained. The scour measured was due to a general beach draw down that also happened in the equivalent test case (T03) without a vertical seawall. Hughes and Fowler (1990) is therefore discounted as a useful basis for determining a fitted expression for scour depth (although it remains useful as a validation test case for numerical modelling).

Fowler (1992) provides the best data set for planar, sloping beaches. However, the beach slope of 1:15 is quite steep compared to a natural sand beach and the range of toe depths was quite limited ($-0.34 \leq h_t/H_s \leq 0.59$). The results are shown in detail in Figure 8 and in a broader context in Figure 10. One limitation of Fowler's data is that it occupies a limited range of relative wave steepness ($0.04 \leq H_s/L_m \leq 0.07$) and relative toe depth ($-0.35 \leq h_t/H_s \leq 0.59$). The range of steepness was intended to model the range found in erosive storms. It seems not to have been enough to determine the variation of scour depth with period. A broader range of relative depth should be modelled using a broader range of frequencies.

Three vertical seawall scour tests were conducted during SUPERTANK (Kraus and Smith, 1994). These were at sufficient scale to avoid scale effects. SUPERTANK results are difficult to use in developing empirical or parametric scour plots as they involved complex bathymetries and involved short bursts of sometimes different conditions, so it is unlikely that equilibrium conditions were reached often. The more complicated SUPERTANK results (from tests ST_70 and ST_80) indicate that local conditions should probably be used to derive empirical scour predictors, rather than offshore conditions, and that developing numerical models of scour may be the best long-term approach.

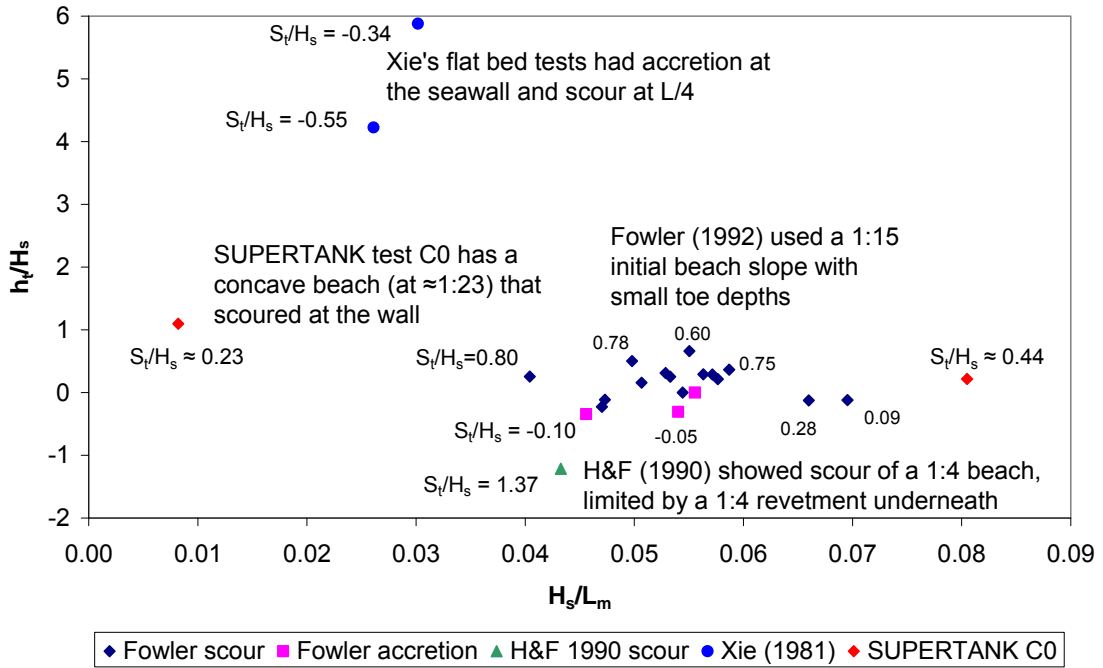


Figure 11 Summary of large-scale scour experiments with irregular waves on parametric scour plot axes.

The foregoing analyses of previous experiments and seawall types have been used to focus the required outcomes of new experiments. The proposed test programme is described in the next section of the report.

6. Physical Model Facility

The tests will be carried out in one of the new 1.2m wide, 1.7m deep, 45m long wave flumes in the Froude Modelling Hall at HR Wallingford. Each flume is equipped with a piston-type wavemaker that can generate waves at water depths of up to 1.4m and has an absorption system for absorbing wave energy reflected from the seawalls. The offshore bathymetry will be moulded in concrete and the test section will consist of a 0.3m deep sand bed at the offshore end, increasing in depth according to the beach slope. The sand bed should be at least 5m long and will potentially need to be $2H_s$ deep near the structure. As the significant wave height will be at least 0.2m, it follows that the sand bed should be at least 0.4m deep at the wall. Table 8 shows possible sand bed lengths and depths for given slopes, as well as the volume and weight of sand required (using a conservative estimate for bed density of 1.9 tonnes per metre cubed).

Table 8 Volume and mass of sand required for different beach configurations

| Length of bed [m] | Beach slope 1:N | Offshore depth of bed [m] | Inshore depth of sand bed [m] | Volume of sand [m ³] | Mass of sand [kg] |
|-------------------|-----------------|---------------------------|-------------------------------|----------------------------------|-------------------|
| 5 | 0 | 0.2 | 0.20 | 1.20 | 2,280 |
| 5 | 50 | 0.2 | 0.30 | 1.50 | 2,850 |
| 5 | 30 | 0.2 | 0.37 | 1.70 | 3,230 |
| 5 | 20 | 0.2 | 0.45 | 1.95 | 3,705 |
| 10 | 0 | 0.2 | 0.20 | 2.40 | 4,560 |
| 10 | 50 | 0.2 | 0.40 | 3.60 | 6,840 |
| 10 | 30 | 0.2 | 0.53 | 4.40 | 8,360 |
| 10 | 20 | 0.2 | 0.70 | 5.40 | 10,260 |
| 5 | 0 | 0.3 | 0.30 | 1.80 | 3,420 |
| 5 | 50 | 0.3 | 0.40 | 2.10 | 3,990 |
| 5 | 30 | 0.3 | 0.47 | 2.30 | 4,370 |
| 5 | 20 | 0.3 | 0.55 | 2.55 | 4,845 |

The most practical option seems to be a 5m long sand bed with an offshore depth of 0.3m. Having a 5m long sand bed will be easier to manage than a 10m long bed, yet will give waves some chance to respond to changes in slope before they reach the seawall. This will be particularly important for beach slopes that are not the same as the concrete bathymetry offshore.

A 1:30 beach slope has been chosen as the default beach slope (see Section 7.2.4). This is relatively shallow as fine sand ($d_{50} = 0.11\text{mm}$) will be used and this would naturally form a gentle beach slope. Having a slope like this will allow tests to be run with water levels lower than the toe of the seawall and will allow flatter and steeper beaches to be tested without too great a change in slope at the offshore end of the sand bed. The concrete offshore slope should be 1:30 too, near the sand bed.

The water depth should be sufficiently deep to generate a significant wave height of 0.2m over a range of wave periods even at the lowest depths (with the still water level lower than the structure toe). A water depth of 0.7m should be sufficient for this. This would leave the structure toe for the standard beach at 0.8m above the flume bed. A water depth of 0.6m at the structure toe would give a water depth of 1.4m at the paddle, which is the maximum possible

and only gives a structure freeboard of 0.3m (if the seawall extends to the top of the flume). The planned bathymetry is shown in Figure 12.

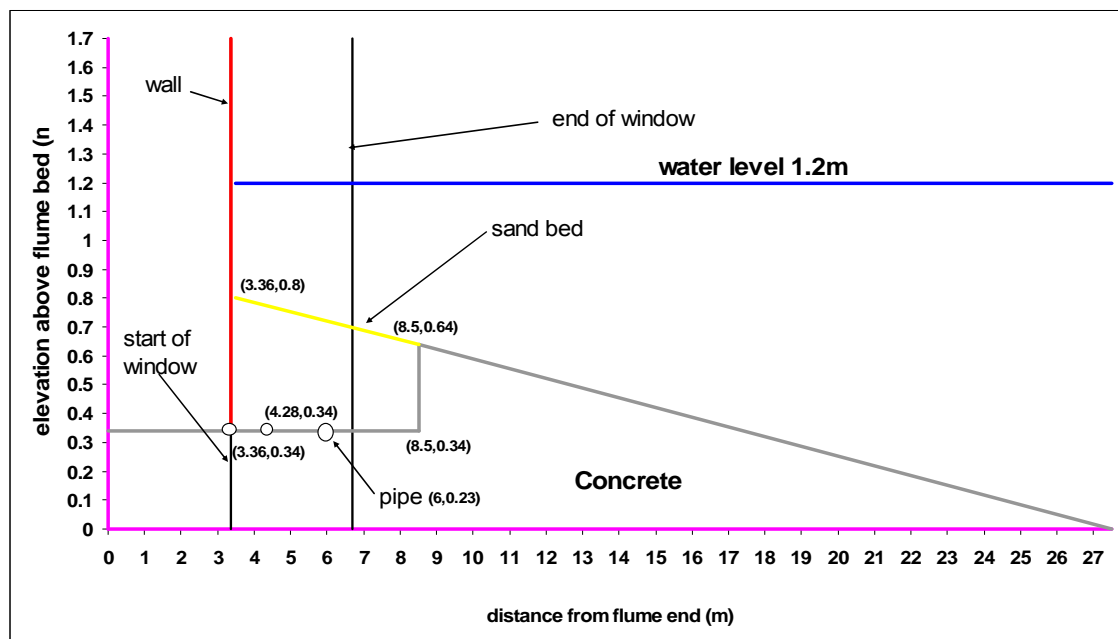


Figure 12 Proposed physical model bathymetry (note distorted scale)

7. Sediment characteristics

The scaling considerations given in Section 3 can lead to the use of sand or lightweight sediment in the physical model. Obviously the smaller the median diameter of sand, the more likely it is to go into suspension. The smallest commercially-available silica sand used by HR Wallingford for sediment transport modelling is Redhill 110, with typically 98.80% SiO₂, 0.09% Fe₂O₃, 0.21% Al₂O₃ and 0.14% LOI (loss on ignition). The results of a sieve analysis of Redhill 110 are shown in Figure 13. The grain sizes, d_n , giving the sieve size that n percent of the sand by weight passes through, are given in Table 9 for common percentiles, such as $d_{16} = 0.087\text{mm}$, $d_{50} = 0.111\text{mm}$ and $d_{84} = 0.154\text{mm}$. Settling velocities are also given for d_{10} , d_{50} and d_{90} from the formulae of Soulsby (1997) and van Rijn (1984), assuming fresh water (salinity = 0) at 15°C, giving density of water $\rho = 999\text{kgm}^{-3}$ and a kinematic viscosity $\nu = 1.141 \times 10^{-6}\text{m}^2\text{s}^{-1}$. In addition, a sediment density $\rho_s = 2650\text{kgm}^{-3}$ was assumed – appropriate for silica sand. This sand formed the basis for the scaling performed in Table 1.

Table 9 Percent by weight passing sieve & fall velocity of Redhill 110 fine sand

| Percent by weight passing sieve | | | Soulsby | Van Rijn |
|---------------------------------|--------|--------|---------------------------|---------------------------|
| (%) | (mm) | (Phi) | w_s (ms ⁻¹) | w_s (ms ⁻¹) |
| 5 | 0.0639 | 3.9691 | | |
| 10 | 0.0742 | 3.7529 | 0.0039 | 0.00435 |
| 16 | 0.0866 | 3.5301 | | |
| 25 | 0.0949 | 3.3980 | | |
| 50 | 0.1114 | 3.1655 | 0.0086 | 0.0085 |
| 75 | 0.1347 | 2.8918 | | |
| 84 | 0.1539 | 2.6999 | | |
| 90 | 0.1667 | 2.5849 | 0.0178 | 0.0175 |
| 95 | 0.1773 | 2.4955 | | |

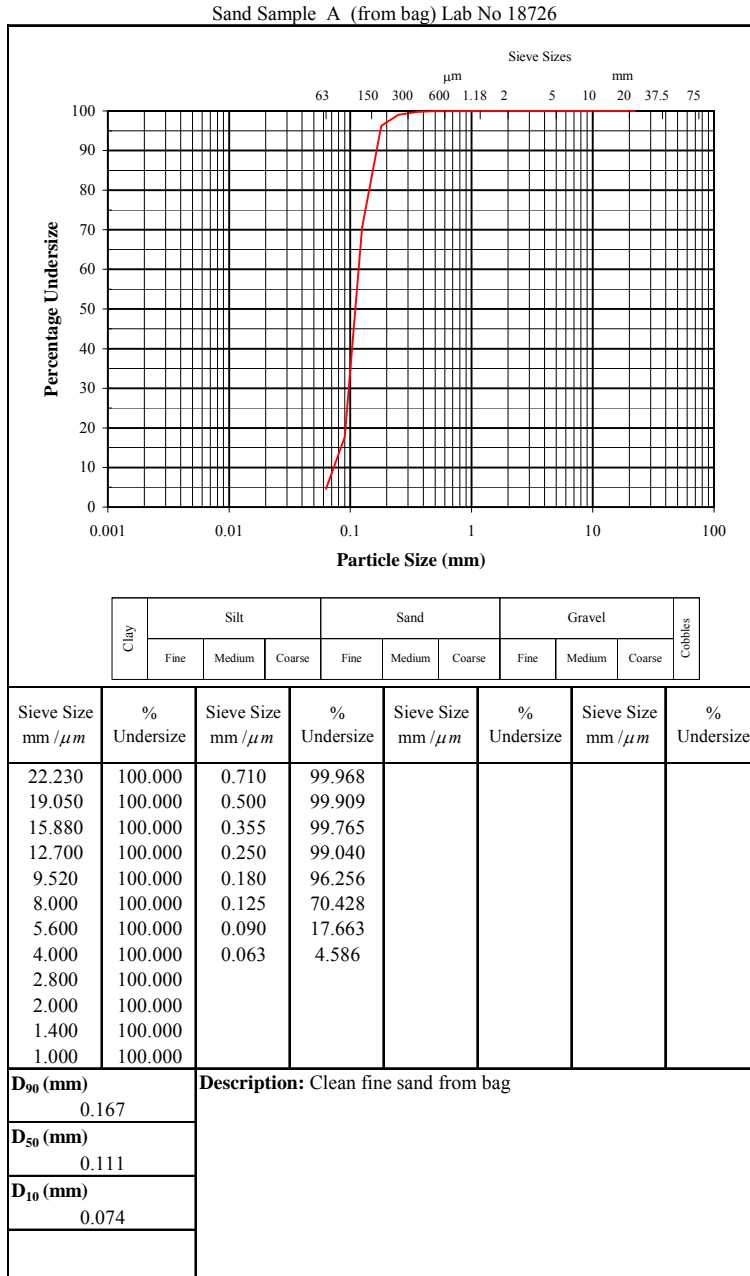


Figure 13 Sediment grading of Redhill 110 fine sand

8. *Design of Test Programme*

8.1 AIMS

The tests have the following aims:

- To provide data to evaluate and improve empirical equations for scour depth based on experiments where suspended sediment transport dominates;
- To test the effectiveness of various toe designs and mitigation measures;
- To provide validation data for numerical models.

8.2 INVESTIGATION OF PARAMETERS

The aims will be addressed by investigating parameters of interest that have been identified from the analyses of previous experiments and aiming to fill gaps in knowledge or resolve uncertainties in existing data. The subsections below detail the sorts of tests that would ideally be carried out.

8.2.1 *Scale Effects*

The arguments presented earlier in this note suggest that if suspended sediment transport is dominant in the physical model tests, the results should be applicable at full scale. In addition the following experiments could be performed to test for scale effects:

1. Repeat conditions at Southbourne (Sutherland and Pearce, 2005). Beach lowering and recovery during a tide were measured at Southbourne in 2005. Wave heights, wave periods and water levels were recorded near the site during the scour measurement period. The most interesting tides could be reproduced in the laboratory at a smaller scale to see if the lowering and recovery of the beach during a tide can be reproduced even though the starting profile must be estimated. This would require varying water levels during the test.
2. Repeat test of Fowler (1992) with 1:15 slope. Repeating a Fowler (1992) test would do less than the other experiments in this list to answer queries about scale effects as it was the closest in scale to the planned tests. However, Fowler (1992) provided more data than any other test series and one of his tests could be repeated to evaluate the effect of beach slope on profile development.
3. Repeat SUPERTANK ST_C0 test. This test was at prototype scale and started with a concave beach slope which averaged about 1 in 23 in the 30m closest to the seawall. It was also the SUPERTANK test which ran for the greatest length of time with a single test condition. This test could be replicated at a smaller scale to see if the profile development is similar.
4. Perform the same test at two different scales in the same test facility. For example, measure scour with $H_s = 0.2\text{m}$, $T_p = 3\text{s}$ and $h_t = 0.4\text{m}$ then repeat with $H_s = 0.05\text{m}$, $T_p = 1.5\text{s}$ and $h_t = 0.1\text{m}$. The processes would be compared through observations of the sediment transport and by comparing the resulting scour profiles, looking at scour depths and the relative importance of ripples, for example.

8.2.2 *Timescale*

Beach profiles will be measured after 300, 1,000, 2,000, 3,000, 6,000 and possibly 10,000 waves to look at timescale of scour. The numbers of waves correspond approximately to the following powers of 10: 2.5, 3, 3.25, 3.5, 3.75 and 4. The scour development will be fitted to the standard

form of timescale function to determine a timescale for scour (e.g. Sumer and Fredsøe, 2002). It will not be necessary to measure all tests at all time intervals.

8.2.3 Wave height, period and depth

Various combinations of H_s , T_p and h_t will be run with the same initial bed slope and structure, to give combinations of h_t/H_s and H_s/L_m that will cover the ranges of Powell and Whitehouse's parametric scour plots (i.e. $H_s/L_m \approx 0.005$ to 0.07 and $h_t/H_s \approx -1$ to 4). The wave height must be kept high to ensure that the sediment near the breakwater is in suspension and it is more straightforward to change wave period than water depth, so a set of tests could be performed at the same h_t and H_s but varying T_p (and hence L_m) to move along the H_s/L_m axis of the parametric plot.

8.2.4 Initial conditions: Bed slope

The effect of beach slope on toe scour is yet to be determined conclusively and has long been a matter of debate. Some researchers have found that varying the initial slope has little or no effect on the final beach profiles, while others suggest that shallower beaches are less vulnerable to toe scour than steeper ones under the same set of wave/water level conditions. Previous tests at HR Wallingford indicate that toe scour depth decreases with a decrease in beach slope angle. This relationship also agrees with the results from other numerical and laboratory studies (McDougal et al., 1996 and Ichikawa, 1967). It is likely that bed slope affects scour processes because it determines the critical wave steepness (which effectively divides breaking and non-breaking sea states) and therefore the way in which the wave breaks. For example, for a given offshore wave height period and water level, waves may break by collapsing and plunging on a steep beach profile; whereas on a shallow shore under the same conditions, the mode of breaking could be spilling. Thus there is likely to be more energy available for scour on steep rather than shallower beaches as the breaker zone reduces in width as the beach steepness increases.

Typical sandy beaches have slopes of 1:20 (2.9°) to 1:30 (1.9°) immediately in front of seawalls, although slopes of 1:15 (3.8°) down to 1:100 (0.6°) are observed. Beach slopes are higher for larger sediment sizes (shingle beaches are typically about 1:8) and tend to flatten offshore. In order to obtain suspension in the laboratory tests a sand with $d_{50} = 0.11\text{mm}$ will be used. This sand would be expected to form a gentle beach slope in nature. The use of a gentle beach slope (1:100 or 1:50, say) in the laboratory tests is likely to cause lower scour depths than a steeper initial bed slope.

A choice must be made between using a gentle beach slope in the laboratory tests (as it is fine sand) and using a steeper bed slope (a typical 1:20 to 1:30, say) which may promote more scour. The use of an over-steep bed (such as the 1:4 bed of Hughes and Fowler, 1990) promotes general offshore sand transport to form a more natural profile, so the original steep profile cannot be recovered by wave action.

In order to investigate the effect of beach slope, a range of tests should be run with different bed slopes to investigate the effect of initial bed slope on final scour profile. At least one set of tests with the same h_t and H_s but varying T_p (and hence L_m) should be run for 3 slopes. These tests need only be run for wave periods that gave significant scour in the initial set of tests (so possibly only 2 or 3 periods per set of tests). Possible slopes include a flat bed (like Xie, 1981), gentle slopes of 1:100 slope or 1:50, typical slopes in the range 1:30 to 1:20 and steep slopes, such as 1:15 slope (like Fowler, 1992). It may be impossible to tell the difference between a flat bed case and a 1:100 slope case so this one could be left out. A flat bed of sand could be used to quantify the limiting case of Xie but might not be directly applicable to beaches. A gentle slope

of 1:50 would provide a contrast to a typical slope that is within the range of observed beach slopes. A slope of 1:25 is in the middle of the typical beach range. A slope of 1:15 is quite steep, but would allow a direct comparison with Fowler (1992).

Therefore, based on the above, the basic beach slope chosen for the first tests will be 1:30, with 1:50 and 1:20 used as low and high slopes to investigate the effect of beach slope on scour.

8.2.5 Initial conditions: Chronology

To test the effects of chronology a set of tests should be run with same water depth, structure and H_s but changing the wave period between tests without re-shaping the sand bed between tests (as above). Profiles should be taken at a number of times to determine the speed at which equilibrium is reached. Then a separate test should be run with the final test wave height and period, but starting from the initial bed configuration. This will determine whether the bed forms a similar final profile and (if so) how quickly it moves towards equilibrium. Recent scour tests using lightweight sediment at the University of Southampton (Pearce, 2005) have indicated that the same final profile may be achieved from a planar initial profile or from the final profile of the previous test, providing that the energy of the incident waves increases from one test to the next.

8.2.6 Overtopping

A further factor of importance may be the extent of any overtopping of the seawall. It is reasonable to expect that seawalls that experience heavy wave overtopping will offer less scour because the proportion of energy reflected or dissipated as turbulence at the wall will be reduced. This effect has probably not been taken into account in previous studies of toe scour, for which the majority of walls appear to have been of sufficient size to limit the extent of any wave overtopping. Thus most empirically based methods for the prediction of toe scour may be conservative if applied to low crest structures, which experience regular overtopping. Similarly, to date, most numerical models can only simulate overtopping by reducing the reflection coefficient for a given seawall profile. Recent developments in phase-resolved modelling of non-linear shallow-water waves (e.g. Dodd, 1998) have allowed wave-by-wave overtopping events to be modelled. Such models could be coupled with sediment transport and bed updating models to investigate the effect of overtopping on scour, although such work is in its infancy. Few, if any, models are able to simulate accurately the turbulent dissipation occurring at the wall.

There are no design relationships to take into account the overtopping influence on scour depth. Nishimura et al., (1978) studied the scour at seawalls caused by an incident tsunami. In this case the overtopping water returned down the face of the structure and much of the scour was caused by the return flow. They noted that:

Scour depth decreases with decreasing wave height and increasing crown elevation (as there is less return flow) however, the area of serious scouring is displaced towards the seawall in this case;

Scour increases (and it occurs at the toe precisely) when the face slope is mild;

Scour decreases markedly when the water depth at the seawall increases;

When waves are applied repeatedly, much less scouring is induced by each successive wave.

A tsunami is not a test case that is normally considered in design, so emphasis should be placed on having at least one test case where there is a significant amount of overtopping without return flow down the face of the seawall. The experiment should be designed to allow the measurement of overtopping and its collection and return.

8.2.7 Seawall type

Most tests will be performed with a vertical seawall as this is generally believed to cause the greatest amount of scour (excluding tsunamis). The same set of tests should be run for different wall slopes as this will affect the amount of energy reflected and the position of the nodes and anti-nodes in front of the structure. The increasing use of rubble mound structures indicates the potential importance of deriving proper design guidance for the toes of rubble mound breakwaters, so that they withstand scour.

8.2.8 Toe protection

Toe protection schemes for seawalls are often relatively simple mattresses or small berms of rock at the toe of the seawall. Tests should be performed to determine the stability of such scour protection so that a design relationship can be determined.

9. Outline Physical Model Test Programme

Select a baseline beach slope and significant wave height. Estimated values are $m = \tan(\alpha) = 0.033$ and $H_s = 0.20\text{m}$. In each case the bed profile will be measured before the test and at stages during the test to determine the development of scour.

9.1 SERIES 1

Test series 1 will test the general behaviour of scour depth with period through the following five tests, which will be run one after the other without recreating the original beach profile. Details of Series 1 tests are provided in Table 10 and Figure 14.

- Test 1 Select a relative depth that is expected to generate significant scour, such as $h_t/H_s = 1$. Set a short wave period, so that wave steepness $s = 0.06$ and $H_s/L_m = 0.1$. Measure the time development of scour.
- Test 2 will be a repeat of Test 1, but with a larger wave period (so larger wavelength and smaller H_s/L_m and $k_p h$) so that $H_s/L_m = 0.06$.
- Test 3 will be a repeat of Test 2, but with a larger wave period so that $H_s/L_m = 0.04$.
- Test 4 will be a repeat of Test 3, but with a larger wave period so that $H_s/L_m = 0.02$.
- Test 5 will be a repeat of Test 4, but with a larger wave period so that $H_s/L_m = 0.01$. This condition can be achieved using $H_s = 0.20\text{m}$ and $T_p = 4.58\text{s}$ or with $H_s = 0.15\text{m}$ and $T_p = 4.0\text{s}$. The latter will be easier to generate in the flume so is likely to be used, possibly at the same water depth as the other tests.

Results from Series 1 will be used to determine the duration of other test series. For example it may be decided to run all subsequent tests for 3,000 waves, like Powell and Whitehouse (1998) rather than attempting to establish an equilibrium condition. The duration of tests will depend on the timescale of scour and the likely duration of storms (including the effect of tides).

9.2 SERIES 2

Test series 2 will investigate the effect of varying toe depth by running the same H_s and T_p at different water levels.

- Test 6 will use the H_s and T_m combination that gave the greatest scour depth in Series 1 (assumed to be $T_m = 4\text{s}$ in Table 10) but will generate the waves at a high water level to give $h_t/H_s = 3$.
- Test 7 will be a repeat of Test 6 with $h_t/H_s = 2$;
- Test 8 will be a repeat of Test 7 with $h_t/H_s = 1$ (i.e. will repeat a test from series 1 from a different starting condition). The similarity of form will give an indication of the importance of starting conditions;
- Test 9 will be a repeat of Test 8 with $h_t/H_s = 0$;
- Test 10 will be a repeat of Test 9 with $h_t/H_s = -0.5$. The precise water level to be used will be decided on wave calibration to ensure that waves will reach the seawall. This test may not work if too much sand has previously been moved offshore.

9.3 SERIES 3

Test series 3 will repeat the form of Test series 1 at a different water depth (probably $h_t/H_s = 2$):

- Test 11 will use $H_s = 0.2\text{m}$ and $T_p = 1.46\text{s}$ at a toe depth $h_t = 0.2\text{m}$ so $H_s/L_m = 0.10$.
- Test 12 will use $H_s = 0.2\text{m}$ and $T_p = 1.87\text{s}$ at a toe depth $h_t = 0.2\text{m}$ so $H_s/L_m = 0.06$.
- Test 13 will use $H_s = 0.2\text{m}$ and $T_p = 2.29\text{s}$ at a toe depth $h_t = 0.2\text{m}$ so $H_s/L_m = 0.04$.
- Test 14 will use $H_s = 0.2\text{m}$ and $T_p = 3.24\text{s}$ at a toe depth $h_t = 0.2\text{m}$ so $H_s/L_m = 0.02$.
- Test 15 will use $H_s = 0.2\text{m}$ and $T_p = 4.58\text{s}$ at a toe depth $h_t = 0.2\text{m}$ so $H_s/L_m = 0.01$.

9.4 SERIES 4

Test series 4 will repeat the form of Test series 1 at a different water depth (probably $h_t/H_s = 0$):

Test 16 will use $H_s = 0.2\text{m}$ and $T_p = 1.46\text{s}$ at a toe depth $h_t = 0.0\text{m}$ so $H_s/L_m = 0.10$.

Test 17 will use $H_s = 0.2\text{m}$ and $T_p = 1.87\text{s}$ at a toe depth $h_t = 0.0\text{m}$ so $H_s/L_m = 0.06$.

Test 18 will use $H_s = 0.2\text{m}$ and $T_p = 2.29\text{s}$ at a toe depth $h_t = 0.0\text{m}$ so $H_s/L_m = 0.04$.

Test 19 will use $H_s = 0.2\text{m}$ and $T_p = 3.24\text{s}$ at a toe depth $h_t = 0.0\text{m}$ so $H_s/L_m = 0.02$.

Test 20 will use $H_s = 0.2\text{m}$ and $T_p = 4.58\text{s}$ at a toe depth $h_t = 0.0\text{m}$ so $H_s/L_m = 0.01$.

Details of test conditions during Series 1 to 4 are shown in Table 10 and Figure 13

Table 10 Test Series 1 to 4

| Series | Test | H_s (m) | h_t (m) | T_p (s) | s | H_s/L_m | h_t/H_s |
|--------|------|-----------|-----------|-----------|-------|-----------|-----------|
| 1 | 1 | 0.2 | 0.2 | 1.46 | 0.060 | 0.099 | 1 |
| 1 | 2 | 0.2 | 0.2 | 1.87 | 0.037 | 0.06 | 1 |
| 1 | 3 | 0.2 | 0.2 | 2.29 | 0.024 | 0.04 | 1 |
| 1 | 4 | 0.2 | 0.2 | 3.24 | 0.012 | 0.02 | 1 |
| 1 | 5 | 0.2 | 0.2 | 4.58 | 0.006 | 0.01 | 1 |
| 2 | 6 | 0.2 | 0.6 | 4.58 | 0.006 | 0.01 | 3 |
| 2 | 7 | 0.2 | 0.4 | 4.58 | 0.006 | 0.01 | 2 |
| 2 | 8 | 0.2 | 0.2 | 4.58 | 0.006 | 0.01 | 1 |
| 2 | 9 | 0.2 | 0 | 4.58 | 0.006 | 0.01 | 0 |
| 2 | 10 | 0.2 | -0.1 | 4.58 | 0.006 | 0.01 | -0.5 |
| 3 | 11 | 0.2 | 0.4 | 1.46 | 0.060 | 0.099 | 2 |
| 3 | 12 | 0.2 | 0.4 | 1.87 | 0.037 | 0.06 | 2 |
| 3 | 13 | 0.2 | 0.4 | 2.29 | 0.024 | 0.04 | 2 |
| 3 | 14 | 0.2 | 0.4 | 3.24 | 0.012 | 0.02 | 2 |
| 3 | 15 | 0.2 | 0.4 | 4.58 | 0.006 | 0.01 | 2 |
| 4 | 16 | 0.2 | 0 | 1.46 | 0.060 | 0.099 | 0 |
| 4 | 17 | 0.2 | 0 | 1.87 | 0.037 | 0.06 | 0 |
| 4 | 18 | 0.2 | 0 | 2.29 | 0.024 | 0.04 | 0 |
| 4 | 19 | 0.2 | 0 | 3.24 | 0.012 | 0.02 | 0 |
| 4 | 20 | 0.2 | 0 | 4.58 | 0.006 | 0.01 | 0 |

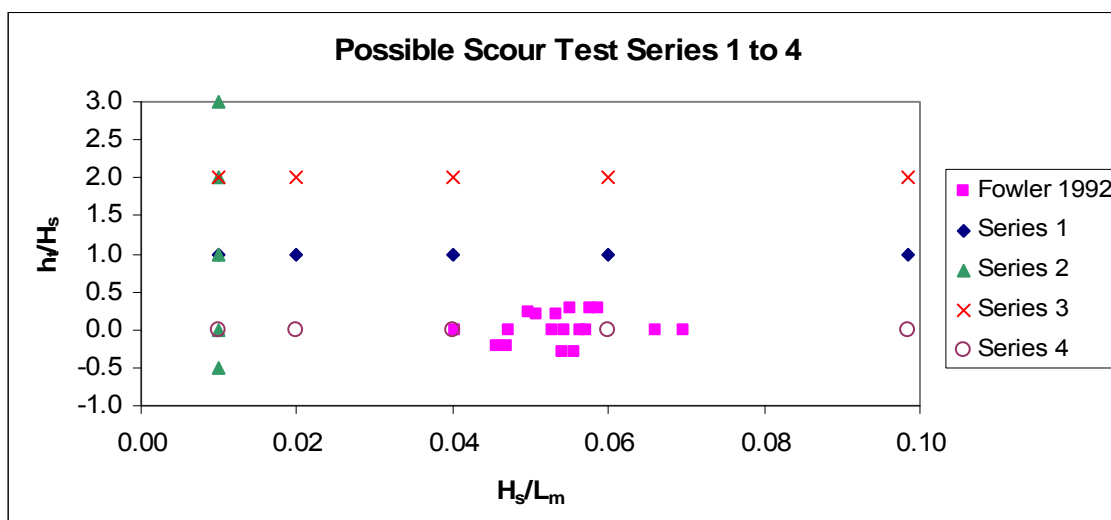


Figure 14 Series 1 to 4 with data from Fowler (1992).

Test Series 1 to 4 will give a good indication of scour behaviour over a wide range of the main parameters for a 1:30 beach.

9.5 TEST SERIES 5 AND 6

Test series 5 would repeat the earlier test series that gave the greatest scour for a gentle bed (proposed to be 1:50). Test series 6 would repeat the earlier test series that gave the greatest scour for a steeper bed (with 1:20 proposed). If time permits, tests will be done with a 1:15 bed as well.

9.6 TEST SERIES 7

Test series 7 will examine the stability of rock armour used as toe protection. A test condition that gave a significant amount of scour will be chosen and rock armour placed at the toe to offer protection. This armour will be chosen so that it should fail at a wave height lower than that chosen. The water depth and wave period from the chosen condition will be used but with a wave height say half that used in the scour test. Waves will be run and any damage measured. The wave height will be increased and damage measured again. This procedure will be repeated until the scour protection fails. The flume may be partitioned into two parallel channels for these tests to allow two different rock sizes to be tested simultaneously. Different hydrodynamic conditions will be tested. Different rock berm heights and widths may also be tested.

9.7 DISCUSSION

Test Series 1 to 4 will allow a systematic testing of the variation in scour with wave period and relative water depth. Test Series 5 and 6 will allow the effects of beach slope to be quantified. However, Fowler's (1992) data showed rapid variations in scour depth with H_s/L_m and h_t/H_s whilst the test series proposed here is relatively widely spaced in H_s/L_m and h_t/H_s and does not pick up on all the details that Fowler (1992) covered. However, a finite set of tests must be made and the proposed approach covers a wider range of the key variables than any other medium scale laboratory scour tests identified so far.

There are some parameters identified as being worth investigating that are not covered in the test programme outlined above. These are:

Scale effects;
Overtopping;
Seawall type.

Direct tests of scale effects, overtopping and seawall type will be made should time permit. One weakness lies in the uniform value of H_s proposed so, for example, H_s/d_{50} will be the same for all tests. Therefore a set of sensitivity tests will probably be carried out after Test Series 2. This could include one test with a reduced freeboard and a second test at a different scale. Tests using a different seawall slope and a different sediment size are intended, although such changes will require considerable work to put into place, so may be left to the end of the test programme.

A period of time at the end of the test programme will be devoted to studying the stability of different scour mitigation measures, primarily rock aprons and rock toes.

9.8 SUMMARY

This Technical Note summarises the arguments made in the design of the physical model tests and in doing so draws heavily on Sutherland et al., (2003). It starts with reviews of the scaling arguments for physical model tests and of previous relevant medium to large scale experiments on scour in front of coastal defence structures. The new wave flumes at HR Wallingford are then described, to indicate the range of parameters for which experiments can be performed. The aims of the test programme and the range of parameters that should be investigated are then described and a systematic test programme is proposed. Whilst the main aim of the tests is to evaluate methods for scour prediction on sand beaches, the proposed test programme is not intended to be prescriptive and the test programme will be optimised, depending on the results of the previous tests.

The tests are scheduled to occur between 24 October and 23 December 2005, although some tests may occur in January 2006, depending on the prior availability of resources.

10. References

- Barnes, T., Brocchini, Peregrine, D.H. and Stansby, P., (1996) Modelling post-wave breaking turbulence and vorticity. *Proc. 25th Int Conf on Coastal Engng*, Orlando, Florida, USA, 1754 – 1768.
- Barnett, M. (1987) Laboratory study of the effects of a vertical seawall on beach profile response. Report 87/005, Coastal and Oceanographic Engineering department, University of Florida, Gainesville, Fl., USA.
- Chesnutt, C.B. and Schiller, R.E. (1971) *Scour of simulated Gulf Coast sand beaches due to wave action in front of sea walls and dune barriers*. COE Report No. 139. TAMU-SG-71-207. Texas A&M University, College Station, TX.
- Carter, T.G., Liu L.-F.P. and Mei, C.C. (1973) Mass transport by waves and offshore sand bedforms. *ASCE Journal of Waterway, Port, Coastal and Ocean Engineering*, 99(WW2): 165-184.
- Dean, R.G. (1985) Physical modelling of littoral processes in *Physical Modelling in Coastal Engineering*, AA Balkema, Rotterdam, 119-139.
- Dette, H.H., Larson, M., Murphy, J., Newe, J., Peters, K., Reniers, A. and Steetzel, H. (2002) *Coastal Engineering* 47, pp 137-177. Elsevier.
- Dette, H.H., Peters, K. and Newe, J. (1998) *Large wave flume experiment '96/97 – experiments on beach and dune stability*. Report No.830, data documentation. MAST III – SAFE Project. Performance of soft beach systems and nourishment measures for European coasts. Commission of the European Union Directorate General XII under MAST contract MAS3-CT95-0004. Leichtweiss-Institute.
- Dodd, N. (1998) Numerical Model of Wave Run-up, overtopping and regeneration. *J. Waterway, Port, Coastal and Ocean Eng.* 124(2): 73-81.
- Fowler, J.E. (1992) *Scour problems and methods for prediction of maximum scour at vertical seawalls*. Technical Report CERC-92-16, U.S. Army Corps of Engineers, Waterways Experiment Station, 3909 Halls Ferry Road, Vicksburg, MS.
- Hughes, S.A., (1993) *Physical models and laboratory techniques in coastal engineering*, World Scientific, pp568.
- Hughes, S.A. and Fowler, J.E. (1990) *Midscale physical model validation for scour at coastal structures*. Technical Report CERC-90-8, US Army Corps of Engineers, CERC, Vicksburg, Miss.
- Hughes, S.A. and Fowler, J. E. (1991) Wave-induced scour prediction at vertical walls. *Proceedings Coastal Sediments*, vol 2. pp1886-1900.
- Ichikawa, T. (1967) Scouring damages at vertical wall breakwaters of Tagonoura Port. *Coastal Engineering in Japan*, vol 10 pp 95-108.
- Irie, I. and Nadaoka, K. (1984) Laboratory reproduction of seabed scour in front of breakwaters. *Proc 19th ICCE*, Houston. ASCE 1715-1731.

- Kamphuis, J.W. (1985) On understanding scale effect in coastal mobile bed models in *Physical Modelling in Coastal Engineering*, AA Balkema, Rotterdam, 141-162.
- Komar, P.D. and Miller, M.C. (1974) Sediment threshold under oscillatory water waves. *J. Sediment. Petrol.* 43, 1101-1110.
- Kraus, N.C. and McDougal, W.G. (1996) The effects of seawalls on the beach: Part 1 - An updated literature review. *Journal of Coastal Research*, vol 12, no. 3 - pp 691-701.
- Kraus, N.C. and Smith, J.M. (editors), (1994) *SUPERTANK Laboratory data collection project. volume 1: Main text*. Technical report CERC-94-3, US Army Corps of Engineers Waterways Experiment Station, Coastal Engineering Research Center, Vicksburg. Miss.
- Kraus, N.C., Smith, J.M. and Sollitt, C.K., (1992) SUPERTANK Laboratory Data Collection Project, *Proceedings of 23rd Coastal Engineering Conference*, American Society of Civil Engineers, 2191 – 2204.
- Longuet-Higgins, M.S., (1953) Mass transport in water waves. *Phil. Trans. Of Royal Soc., London, series A*, 245: 535-581.
- Loveless, J.H. and Grant, G.T. (1994) Physical Modelling of Scour at Coastal Structures. HYDRA 2000, *Proceedings of 26th Congress of Int. Assoc. for Hydraulic Research*. (3): 293-298 ISBN 0-727-72056-2.
- McDougal, W.G., Kraus N.C. and Ajiwibowo, H. (1996) The effects of seawalls on the beach: Part II, numerical modelling of SUPERTANK seawall tests. *Journal of Coastal Research*, vol 12, no. 3, pp 702-713.
- Nishimura, H., Waranoke, A. and Horikawa, K. (1978) Scouring at the toe of a seawall due to tsunamis. *Proc. 16th Coastal Engineering Conference*, Hamburg, Germany, ASCE 2540-2547.
- O'Donoghue, T. and Sutherland, J., (1999) Random wave kinematics and coastal structures. *Proc. Instn Civ. Engrs Wat, Marit. & Energy*. 136: 93-104.
- Oumeraci, H., (1994) Scour in front of vertical breakwaters – review of problems. Proceeding Int Workshop on *Wave barriers in deepwaters*. PHRI, Yokosuka, Japan.
- Owen, M.W. (1980) *Design of seawalls allowing for overtopping*. HR Wallingford Report EX 924.
- Pearce, A.M.C., 2005. Personal communication about PhD at University of Southampton.
- Pedersen, C., Deigaard, R. and Sutherland, J. (1998) Measurements of the vertical correlation in turbulence under broken waves. *Coastal Engineering*, 35, 231 – 249.
- Powell, K.A. and Lowe, J. P. (1994) The scouring of sediments at the toe of seawalls. In: *Proceedings of the Hornafjordur International Coastal Symposium*, Iceland - June 20-24. Edited by Gisli Viggoisson - pp 749 to 755.
- Powell, K.A. and Whitehouse, R.J.S. (1998) The occurrence and prediction of scour at coastal and estuarine structures. *33rd MAFF Conference of River and Coastal Engineers*, 1-3 July 1998. Keele University. UK.

Sakakiyama, T. and Kajima, R. (2002) Experimental study on toe scour of seawall covered with armor units due to waves. *First International Conference on Scour of Foundations*, ICSF-1, Texas AandM University, College Station, Texas, USA. Nov 17-20.

Smith, J.M. and Kraus, N.C. (editors), (1994) *SUPERTANK Laboratory data collection project. volume II: Appendices A – I.* Technical report CERC-94-3, US Army Corps of Engineers Waterways Experiment Station, Coastal Engineering Research Center, Vicksburg, Miss.

Soulsby, R.L., (1997) *Dynamics of Marine Sands* Thomas Telford, London. ISBN 07277 2584 X.

Sumer, B.M., (1986) Recent developments in the mechanics of sediment suspension. *Proc Euromech 192: transport of suspended solids in open channels*. Neubiberg, Germany. AA Balkema publisher, The Netherlands, 3-13.

Sumer, B.M. and Fredsøe, J. (2000) Experimental study of 2D scour and its protection at a rubble-mound breakwater. *Coastal Engineering*, vol 40. 5-87. Elsevier Science.

Sumer, B.M. and Fredsøe, J., (2002) *The mechanics of scour in the marine environment*. World Scientific, pp536.

Sutherland, J. (1999) Morphodynamic research in coastal wave basins. *Proc Hydralab workshop – Experimental research and synergy effects with mathematical models* 49-58.

Sutherland, Brampton, Motyka, Blanco and Whitehouse, (2003) *Beach lowering in front of coastal structures, research scoping study*. Defra report FD1916/TR1.

Sutherland and Pearce (2005) *Beach lowering and recovery at Southbourne (2005)*. HR Wallingford Technical Note CBS0726/TN01.

Sutherland, J. and Whitehouse, R.J.S. (1998) *Scale effects in the physical modelling of seabed scour*. Report TR64. HR Wallingford. UK.

Tørum, A., Huhnen, F. and Menze, A. (2003) On berm breakwaters: stability, scour, overtopping. *Coastal Engineering* 49(3) 209–238.

Van der Meer, J W. and Veldman, J.J. (1992) Singular points at berm breakwaters: scale effects, rear, round head and longshore transport. *Coastal Engineering*, Amsterdam. Elsevier Science.

Van Gelder, P.H.A.J.M. and Vrijling, J.K., (2000) On the distribution of the maximum wave height in front of reflecting structures. *Proceedings of Coastal Structures '99*. Losada (Ed) Balkema, pp37 - 46.

Van Rijn, L.C. (1984) Sediment Transport. *J. Hydraulic Divisions Proc ASCE* V110, pp 1431-1456, 1613 – 1641 and 1733 – 1754.

Xie, S-L. (1981) *Scouring patterns in front of vertical breakwaters and their influence on the stability of the foundations of the breakwaters*. Department of Civil Engineering, Delft University of Technology, Delft, The Netherlands, 61p.

Yalin, M.S., (1963) A model shingle beach with permeability and drag forces reproduced. *10th Congress IAHR, London* (1) 169-175.

